Available online at www.sciencedirect.com

SCIENCE DIRECT®

Biochimica et Biophysica Acta 1711 (2005) 99 – 125

BIOCHIMICA ET BIOPHYSICA ACTA
BBA

http://www.elsevier.com/locate/bba

Review

Structural organization of gap junction channels

Gina E. Sosinsky[a], Bruce J. Nicholson[b,*]

[a]*National Center for Microscopy and Imaging Research, Department of Neurosciences, University of California San Diego, La Jolla, CA 92093-0608, USA*
[b]*Department of Biochemistry, University of Texas Health Sciences Center, San Antonio, TX 78229-3900, USA*

Received 30 August 2004; received in revised form 22 March 2005; accepted 2 April 2005
Available online 19 April 2005

Abstract

Gap junctions were initially described morphologically, and identified as semi-crystalline arrays of channels linking two cells. This suggested that they may represent an amenable target for electron and X-ray crystallographic studies in much the same way that bacteriorhodopsin has. Over 30 years later, however, an atomic solution structural resolution of these unique intercellular pores is still lacking due to many challenges faced in obtaining high expression levels and purification of these structures. A variety of microscopic techniques, as well as NMR structure determination of fragments of the protein, have now provided clearer and correlated views of how these structures are assembled and function as intercellular conduits. As a complement to these structural approaches, a variety of mutagenic studies linking structure and function have now allowed molecular details to be superimposed on these lower resolution structures, so that a clearer image of pore architecture and its modes of regulation are beginning to emerge.

Keywords: Gap junction; Connexin; Structure; Mutagenesis; Electron microscopy; NMR; Atomic force microscopy; Pore structure; Gating

Contents

* Corresponding author.
E-mail address: nicholsonb@uthscsa.edu (B.J. Nicholson).

0005-2736/$ - see front matter © 2005 Elsevier B.V. All rights reserved.
doi:10.1016/j.bbamem.2005.04.001

Gap junctions represent a ubiquitous component of all multicellular animals and serve important functions in direct intercellular communication between most cell types in all metazoan species. However, despite the conserved structure, properties and possibly functions of gap junctions in both vertebrates and invertebrates, these structures have evolved independently, with topologically analogous, but unrelated protein families (connexins [1], innexins [2], respectively). The innexin family is likely to be the most ancient, as relatives, termed the pannexins, are found in mammals [3]. However, connexin based gap junctions have been studied in far more detail, and it is these structures that will be discussed in this chapter. Gap junctions play a dynamic role in developmental regulation and signal transduction pathways using classic signaling molecules such cAMP and other nucleotides, calcium ions, and inositol triphosphate [4–6] as well as providing a direct pathway for metabolites [7,8] that mediate cell homeostasis, and ions that propagate electrical signals in the heart [9] and the nervous systems [10]. These small molecules and ions diffuse passively through gap junction channels that span the bilayers of both cells and the extracellular "gap", or space, that separates them. However, as described below, the specific connexin composition imparts significant specificity to the signals that can pass.

Mutations in connexin genes have been demonstrated to be the cause of several diseases such as X-linked Charcot–Marie–Tooth syndrome (CMTX, a peripheral neuropathy, [11,12]); nonsyndromic sensineural deafness [13]; several skin diseases [14]; cataracts [15,16] and ODDD (Oculodentodigital or oculodentoosseous dysplasia, a rare pleiotropic disorder mainly with ocular, craniofacial and digital anomalies and, sometimes with late onset, neurological manifestations, [17]). Elucidating the effect of these naturally occurring mutations in diseases has provided motivation for understanding the role single site amino acid substitutions play in the molecular basis of connexin diseases (often referred to as connexin-opathies). In turn, this has also increased the interest in defining the structure of the gap junction channel at the molecular level so that the larger context of these mutants can also be understood.

Understanding the functionality of gap junctions and its constitutive proteins by interpreting its molecular structure remains a complex problem, contributed to by the multiplicity of connexins (>20 to date) with differing physiological properties and regulatory features. However, the multiplicity of connexins also aids in the design of structure/function studies because comparative sequence analysis can be useful in identifying important residues. It is also important to point out that while structural studies can identify static channel conformations, it is critical to correlate and integrate this structural information with dynamic functional studies from electrophysiology, selectivity assays and signal transduction experiments to validate whether these structural conformations correspond to functional states.

The primary direct structure determination tool that has been used to obtain three-dimensional information has been electron crystallography. However, these studies have been limited to only a few connexins, have provided only one structure at less than 10 Å resolution and also present only a static representation of the gap junction. Recently, other techniques have yielded information about connexin structure and dynamics that provide a bigger picture of connexin organization and domain movements. In this review, we present these new data in the context of structures and structural models deduced from topological mapping (Fig. 1A), electron microscopy (EM, Fig. 1F and I) and X-ray diffraction of the proteins. Information from nuclear magnetic resonance spectroscopy (NMR) of small soluble domains of connexin peptides in solution has provided insights into the cytoplasmic structure that in general appears to be highly disordered (Fig. 1B, C and E). Atomic force microscopy (AFM) imaging (Fig. 1D and H) and surface plasmon spectroscopy (SPS) studies published within the last 3 years have probed the dynamics and flexibility of the accessible surface structures of connexins. All of these studies are complemented at the molecular level by mutagenic, biochemical and expression studies that have defined the functional significance of several domains and provided some surprising structural insights (e.g., Fig. 1G).

The term "gap junction" comes from histological studies done in the 1960s [18] and describes their appearance in the first electron microscopy studies using heavy metal incubations. These distinct morphological areas are found in almost all tissues in which cells abut each other. Lanthanum could be used to infiltrate the extracellular regions, creating the appearance of a distinct space or 'gap' between the two plasma membranes. This was in contrast to structures called tight junctions, where the lanthanum failed to penetrate. In thin sections, stain also outlined striations running perpendicular to and connecting the two plasma membranes [19]. Subsequent freeze-fracture and thin-section electron micrographs showed that these striations arose from packed arrays

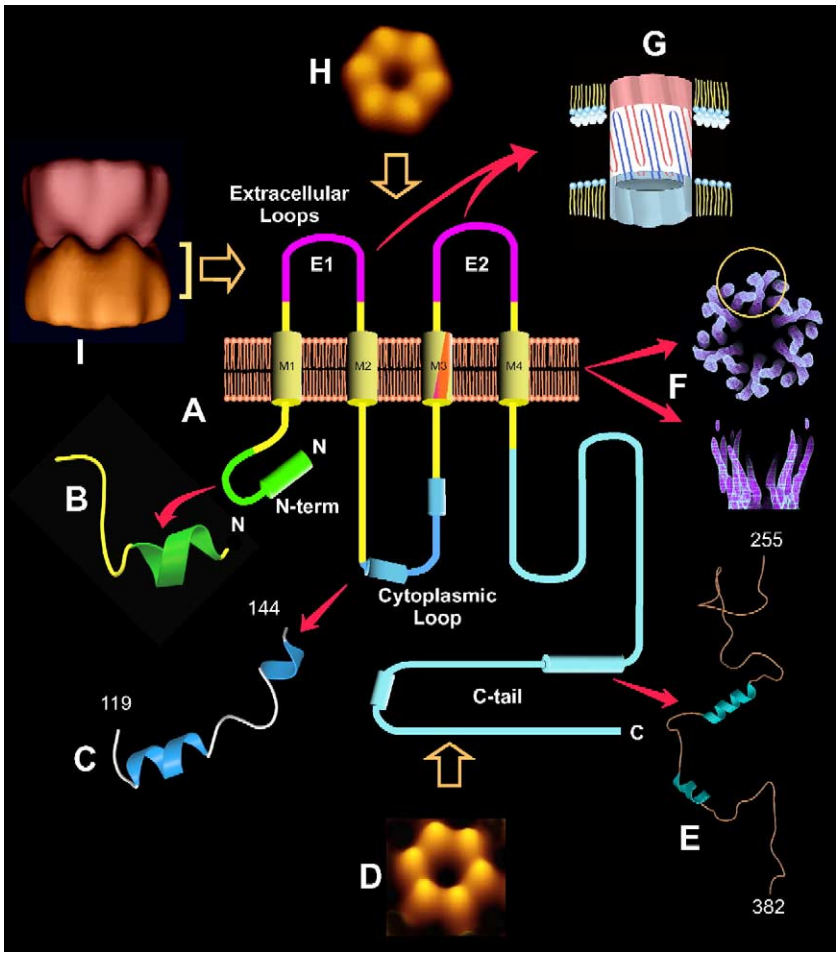

Fig. 1. Composite of information on the structure of gap junction channels. This montage of images illustrates the present knowledge about the appearance of the various domains of connexin channels. (A) The central figure is a topology diagram of a generic connexin monomer. (B) N-terminus secondary structure from the NMR structure determination of the Cx26 N-terminus peptide [131]. (C) Secondary structure of a peptide with the sequence of a portion of the cytoplasmic loop of Cx43 as determined by NMR [133]. (D) Topographic structure of the cytoplasmic domains of Cx26 as imaged by AFM [93]. (E) Structure of a peptide with the sequence of a portion of the carboxy terminus of Cx43 as determined by NMR [150]. Note how each of the structures shown in (B), (C) and (E) contain the motif of short α helices connected by varying lengths of random coil. (F) 3D structure of the α helical transmembrane domains seen perpendicular (top) and parallel (bottom) to the membrane plane as determined by e^- diffraction of truncated Cx43. One possible arrangement of helices within a subunit is circled in top panel [29]. (G) Model of the double β barrel architecture in the extracellular domains as deduced by mapping of disulfides though mutagenesis [33]. (H) Topographic structure of the extracellular domains of Cx26 in a Ca^{2+} free state as imaged by AFM [93]. (I) 3D model of a full gap junction channel obtained by computationally docking a 3D reconstruction of a connexon with a symmetry-related partner connexon to show the interdigitation of the connexons at the extracellular surface [114].

of hundreds to thousands of intercellular channels that directly connect the cytoplasm of one cell with the cytoplasm of a neighboring cell [7,20–23]. Today, the term "gap junction" refers to these plaques or maculae containing multiple intercellular channels spanning the two plasma membranes and the narrow extracellular "gap" that separates them.

1. Early biochemical studies

1.1. Domain organization of gap junction channels (topology models)

Vertebrate gap junction channels contain one or more different proteins from a multigene family of homologous proteins called *connexins*. The connexin proteins are designated by the abbreviation *Cx* followed by the molecular weight in kilodaltons, e.g., Cx26 for connexin26. Species differences are denoted by a single letter at the start of the name, e.g., hCx43 for human connexin43. Based on primary sequence similarities, the connexins are predicted to share a common folding topology [24]. Early proteolysis and antibody susceptibility studies of these preparations have shown that the protein chain traverses the membrane four times [25,26] and these experimental studies were further supported by hydropathy analyses [27,28]. The four transmembrane segments were predicted to be α helices based on the number and nature of the constitutive amino acids in each segment. The N and C termini, as well as the loop connecting the second and third transmembrane helices, are located on the cytoplasmic side of the cell

membrane while the extracellular (or gap) side of the membrane contains the two loops that connect the first to the second transmembrane helix and the third to the fourth transmembrane α helix (Fig. 1A). A high-resolution (~7 Å) structure of a truncation mutant of Cx43 [29] validated this hypothesis (Fig. 1F). A higher resolution structure, 5.7 Å in plane, 19.8 Å perpendicular to the membrane plane, based on further refinement and analysis of the data from the ~7 Å structure, has recently been published [30]. This structure contains the same basic design of the original structure, but with better definition of the transmembrane helices. Comparisons of the amino acid sequences of various connexins have shown that the four membrane spanning domains and the two extracellular loops are the most conserved domains, while the most variable sequences are found in the cytoplasmic central loop and C-terminal domain (Fig. 1A).

The connexon, a hexamer of connexins within one cell (often referred to as a hemichannel), can be thought of as consisting of three functional domains: the transmembrane domains that form the channel; the extracellular domains that are important in cell–cell recognition and docking of the two connexins, as well as contributing to the extracellular portion of the pore, and; the cytoplasmic domains that influence the physiological/gating properties of the channel. It is important to keep in mind that this is a highly simplistic view because we know that the primary amino acid sequence in the cytoplasmic domains does influence how two connexons come together and dock [31], indicating an inter-dependence between quite distant portions of the structure. However, as is common with many structural studies of proteins, such a domain compartmentalization is useful in thinking about the design of experiments that test the effect of mutations on the trafficking and functionality of these intercellular channel proteins. The four membrane spanning segments (referred to as *TM1*, *TM2*, *TM3* and *TM4*) form a four α-helix bundle, so that when the hexamer is formed, a closed cylindrical structure is obtained [32] with one major helix (and possibly part of a second) from each subunit contributing to the pore lining of the channel. The 7 Å structure contains four transmembrane rods corresponding to α helices [29]. The N terminus (*NT*), the connecting loop between the TM2 and TM3 helices (referred to as the cytoplasmic loop or *CL*) and the carboxyl terminus (*CT*) comprise the cytoplasmic domains. Each connexin contributes two loops (referred to as *E1* and *E2*) to the extracellular domain. The interpretation of results from site directed mutagenesis studies of the extracellular domains are consistent with the hypothesis that upon docking of the two connexons, a complex β sheet arrangement consisting of two concentric β barrels, with three conserved inter-loop disulfide bonds in each connexin connecting them, is formed from the 24 extracellular loops [33] (Fig. 1G). It is important to note that while the term "connexin" and "subunit" are often used interchangeably, these may not necessarily be the same. In 3D reconstructions, organized hexagonal features within the connexon are often referred to as subunits but could be composed of parts of more than one connexin [29].

1.2. Isolation and purification of gap junctions

Several factors complicate the preparation of suitable specimens for structural studies. Due to the tight associations of connexins to maintain the channel structure, as well as the close association between channels, gap junctions are usually isolated as maculae containing the intact channels rather than as soluble proteins. Treatments with chaotropic agents generally separate the two membranes rather than solubilize the channels into monomers [34]. Harsher biochemical treatments, such as treatment with SDS, solubilize the connexons or channels into monomers, but denature the protein. In addition, most tissues studied to date express two or more connexins [35] and few tissues are useable as the starting material. Gap junctions constitute <0.1% of the cell surface, even in the highest expressing tissues such as liver hepatocytes [22] where the predominant connexins are Cx32 and Cx26 in varying proportions among different mammalian species [36,37]. Gap junctions have been isolated from heart tissue [38], rodent liver tissue [39] and lens tissue [40] with yields of 1–10 μg of purified connexin. While these amounts were suitable for EM and early studies using X-ray fiber diffraction, the protein amounts are too small for systematic protein crystallization or NMR structure determination. Recent preparations from gap junctions expressed in tissue culture cells have provided better purity than with tissues [41,42], but still contain <1 mg of protein. Solubilized connexons can also be isolated from more loosely packed structures (plasma membrane fractions) [43–48] for two or three dimensional crystallization studies. However, the goal of preparing useful three-dimensional crystals from these samples for X-ray crystallographic studies has proved elusive [47] and even reconstitution into 2D crystals for high resolution electron crystallographic studies has not yet provided specimens similar in quality to those obtained by membrane purification techniques [47–49]. Finally, in order to study connexins in the context of the in vitro functional unit, one must obtain two docked connexons, or hemichannels, from opposed membranes. It has been very difficult to visualize in vitro conformational changes in isolated gap junctions due both to the difficulty in obtaining good samples and the limited resolution of the two-dimensional crystals when electron crystallographic techniques are used as the primary structure determination method. EM of negatively stained gap junctions and reconstituted single connexon layers is typically used to assay structural integrity and assembly [48].

Early biochemical studies showed that gap junctions could be purified for structural analysis using sucrose

gradient centrifugation, cell fractionation [50,51], high alkali conditions [39] and/or treatments with one or more detergents. In these protocols, the effect of the detergents or alkali is to remove non-essential lipids from the gap junction plaques and solubilize non-junctional plasma membrane fragments [52]. In this context, a non-essential lipid can be defined as one that extracts easily with detergent or alkali treatments from gap junction plaques, structure and functionality are still maintained. During isolation and purification, the membrane channels re-pack from a close packing arrangement to a hexagonal lattice containing nominal p6 symmetry. Depending on the isolation conditions and detergent extraction procedures used, the lattice constant ranges from 74 to 90 Å, with smaller connexins and more ordered lattices exhibiting smaller lattice constants [53]. In situ, the channel-to-channel distance is 95–100 Å [54] and the packing is hexatic in nature [55]. The term "hexatic" refers a state intermediate between the liquid and solid [56]. It was shown that in the membranes of biological cells, a significant fraction of the lipid bilayer is in the hexatic state, and may act as to restrict the mobility of membrane-bound proteins [57].

These clusters of membrane channels exclude other integral membrane proteins, thereby minimizing the amount of surface area necessary to bring the two cells into close apposition [58]. The packing density is altered by the removal of lipids from the spaces between the membrane channels. The protein-to-lipid ratio is completely dependent on the method of isolation and alkali- or detergent-based crystallization [34,59]. Treatments with detergents have been shown to selectively remove the phospholipids, but the cholesterol composition remains about the same [60]. In fact, the cholesterol content of isolated gap junctions is quite high compared to other membranes [59]. The 8° skew of the connexon within the hexagonal lattice first seen by Baker et al. [61] is the direct result of the removal of lipids by the detergents used for crystallization [52] and is not an intrinsic feature of the in vivo connexon or intercellular channel.

Early electron microscopy (EM) studies [62] imaged the membrane channels as two hexamers (connexons or hemichannels) either by thin section or negative staining methodology. The structure is exceedingly sensitive to electron irradiation, and as a result, conventional EM images gap junction channels as arrays of "doughnuts" and significant flattening occurs [61,63]. As imaged by low dose negative staining or frozen-hydrated EM, the membrane channel appears in projection as a skewed, six-lobed unit ~65 Å in diameter [61,64–66]. Two connexons pair to form a tight seal, with a 20- to 30-Å gap between the apposing cell membranes, creating a dimer of two hexamers. Because these early preparations contained two-dimensional crystalline arrangements, gap junctions were considered as early targets for molecular structure determination for the emerging fields of electron crystallography and X-ray fiber diffraction [67,68].

2. Early structural images

2.1. Imaging of multi-connexin gap junction membrane channels

Connexons can be assembled from one connexin (called a *homomeric connexon*) or more than one connexin (called a *heteromeric connexon*). Consequently, an intercellular channel can be composed of two identical *homomeric connexons* (called a *homotypic junction*) or two connexons of different heteromeric or homomeric composition (called a *heterotypic junction*). Mixing of connexins within the channel is hypothesized to be possible because of the high conservation of primary sequence in the extracellular and transmembrane domains [69], however, there is some selectivity as to which connexins partner with others (see Ref. [70] for a recent review describing electrophysiology and dye transfer studies of various heterotypic and heteromeric pairings and for a comprehensive list of allowed and disallowed heterotypic pairings [71]). Recent work strongly suggests that heterotypic junctions can have distinct molecular permeabilities from their parental homotypic junctions. Therefore, a variant pore can form that is suited to the selective passage of different molecules from homotypic or homomeric channels [72]. Indeed, it is becoming increasingly apparent that connexin composition strongly influences the passage of molecules through the pore, related to size, charge and shape of the permeant, the effective pore size and affinities between the pore wall and the permeants, as discussed below [73–76].

Direct imaging of connexin mixing within a gap junction plaque was first shown by Zhang and Nicholson [77] using immunogold labeling of mouse liver plaques, and subsequently has also been shown using freeze-fracture immunolabeling techniques in both isolated gap junctions [37] and gap junction in situ [37,78]. Confocal microscopy has provided a wealth of data showing mixing of connexins in tissues using immunolabeling (e.g. Ref. [79] showing mixing and segregation of Cx43 and Cx26 in epidermis tissue) and lately, using fluorescent tags such as GFP and its spectral variants attached to connexins and expressed in tissue culture cells [80,81]. These fluorescent tags allow for imaging of live cells whereby the ebb and flow of connexins and their gap junction structures can be monitored in real time [80]. In particular, the studies by Falk et al. have elegantly shown that fluorescent tagging, in combination with deconvolution microscopy, pushes the resolution to the theoretical point resolution of ~0.1–0.2 μm typically quoted for fluorescence microscopy [82]. In addition, having the z-dimension in these reconstructions allows for the determination of whether another molecule co-localizes within a plaque or is located just above or below it [82]. Three-dimensional volumes of the deconvolved fluorescence data demonstrate clear separation of Cx43 and Cx32 domains within a single gap junction plaque, as well as complete overlap of fluorescence arising from Cx43 and Cx26 within a large gap junction plaque. However, the

resolution is still insufficient for determining whether the constituent channels are homomeric, homotypic, heterotypic or heteromeric in composition.

The higher resolution technique of Scanning Transmission Electron Microscope (STEM) mass analysis has also been employed to address the question of mixing of connexins within gap junctions [36]. In the STEM, only the elastic ("dark field") signal is collected. This scattering is proportional to the mass density of the object being imaged and can be calibrated with appropriate standards such as tobacco mosaic virus to obtain accurate mass measurements [83]. Using the lattice positions in isolated, 2D crystalline gap junction plaques as a guide for pinpointing where the channel centers are located, the mass of populations of intercellular channels and connexons in mouse liver gap junctions was measured. Analysis of these histograms indicated that heterotypic channels of Cx32 and Cx26 occurred in vivo in isolated gap junction plaques [36], but that heteromeric connexons could not be detected. Clear segregations and mixing could be seen on the molecular level in the intact plaques, while if heteromeric connexons did exist in the split junctions, the populations would be such a minor component that they were not within the detection accuracy. It is important to point out that heteromeric connexons have been isolated from whole lens and liver membrane homogenates in biochemical analyses [44,45], and the differences between these studies may reflect the samples being evaluated (i.e., detergent purified crystals versus whole membrane fractions). However, from the wealth of immunolabeling light microscopy data, it appears that, in tissues, heterotypic junctions and heteromeric connexons are more the exception than the rule in terms of mixing of connexin isoforms. Still, from a structural perspective, it is interesting to think about how to build models that allow for both compatibilities in the pairings at the extracellular surface as well as how bulky, flexible C-termini could interact in heterotypic/heteromeric pairings. Another important point to note is that, while the E2 extracellular loop can be an important determinant of docking specificity [84], there are few amino acid differences in this loop between compatible connexins. Thus, it is likely that small tertiary structural changes can greatly influence which connexin can form heterotypic pairings with other connexins [85].

2.2. X-ray fiber diffraction of partially-ordered pelleted gap junctions: development of the first 3D structural models

In 1970s, X-ray fiber diffraction showed great promise as a technique for structure determination of filamentous viruses, bacteriophages and membranes. The technique has become less used for membrane structures because of difficulties in obtaining well-aligned specimens and interpretation of the complex X-ray diffraction patterns where overlap of the layer lines leads to several non-unique and probable solutions. Meanwhile, X-ray and EM crystallographic structure determination methods have improved to the point where if suitable 3D or 2D crystalline specimens are obtained, a structure can be determined in a year or less. Regardless, it is important to point out that X-ray and electron microscope studies in 1977 by Caspar et al. [67,86] revealed the first 3D structure of the gap junction. Because the resolution of gap junction crystals was limited to ~20 Å for many years, the model derived from the 1977 X-ray and EM analysis has remained the standard representation of gap junction structure.

Analysis of the X-ray diffraction data was useful in characterizing the density and packing distributions of protein in hydrated samples. Alterations in molecular structure were reflected in differences in the meridional diffraction, whereas differences in the equatorial diffraction reflected changes in lattice packing. Comparison of several specimens of partially ordered, stacked, mouse liver gap junctions (containing Cx32 and Cx26) showed a basic, invariant structure in which the cytoplasmic portions of the connexin molecules extend out ~90 Å from the center of the membrane channel [86]. The fiber diffraction analysis of Makowski et al. [86] showed that the extracellular gap was ~35 Å thick, the lipid head-groups were separated by ~45–50 Å, and the lipid tail region of each membrane was ~32 Å thick. A central channel runs through the gap junction with an ~25 Å opening at the cytoplasmic end. It is worth noting that because X-ray scattering from elements such as phosphorous is strong, these studies have provided the only detailed structural measurements of the lipids in the two gap junction plasma membranes. From their analysis, it was clear that gap junctions exhibit short-range disorder coupled with long-range order because high-resolution meridional reflections at ~3–4 Å were clear in their diffraction patterns, while reflections between a resolution range of 20–4 Å were missing or extremely weak. These high resolution reflections could only arise from highly ordered secondary structure while the lack of medium resolution data indicates the disorder inherent in the crystal lattice. The nature of the 3–4 Å data was further studied by modeling and simulating diffraction patterns by Tibbits et al. [87]. In addition, systematic differences between the X-ray patterns of oriented gap junctions pellets in normal and calcium free buffer led Unwin et al. to propose the hypothesis that closure of the channel pore occurred by a tighter packing and more vertical arrangement of the helices in the transmembrane domain [88].

2.3. Early EM 3D reconstructions: 3D structure at ~25 Å resolution

Gap junctions were one of the first membrane proteins to be reconstructed by negative stain and cryo-EM. Three-dimensional reconstructions by Unwin et al. [66,89] showed that the connexon contained a torus with six rod-like subunits oriented perpendicular to the membrane. In their reconstructions, the subunits are ~25 Å in diameter and the

channel opening at the cytoplasmic surface is ~20–25 Å. Reconstructions obtained from samples with and without EGTA showed small differences in pore size, packing and thickness that were interpreted as two functional states. From these data, a model was presented in which the pore of the channel closes via a tilt-rotate process that is analogous to a camera iris mechanism [66,89].

The overall shape of this structure supported the hypothesis obtained from the topology studies that connexins contain significant proportions of α-helical conformation. This was consistent with earlier circular dichroism studies that estimated the α-helical content to be 40–65% depending on the sample preparation conditions [90]. In addition, comparison of X-ray patterns from oriented gap junctions with other solved protein structures indicated that the transmembrane portions of the connexins are significantly α-helical [87]. It was further postulated that the helices span the membrane, with one or more being tilted, and that the helices may extend into the polar lipid headgroups and perhaps even into the gap region, although the latter proposal has not been borne out by the ~7 Å structure of Unger et al. [29].

Missing from all 3D EM crystallographic structures is any significant visualization of the cytoplasmic domains [29,66,89,91]. While crystallographic analysis by X-ray or EM is the most reliable high resolution technique for directly determining atomic structure once a protein is crystallized, the drawback with any technique based on crystal data is that any part of the structure not maintained in the same position and orientation on the crystal lattice from molecule to molecule will appear smeared or missing. The connexin cytoplasmic domains are highly sensitive to beam damage and dehydration conditions [61,63] and all previous structures consisted almost entirely of information from the transmembrane and extracellular domains [92]. Evidence for this hypothesis has come from studies of different connexins and their proteolytically cleaved forms. From thin sections, or edge-on views of negatively stained isolated gap junction pellets, the thickness of the gap junction increases as the cytoplasmic C-terminus increases in length from ~170 Å for Cx26 [93], ~190 Å for Cx32 [63], ~250 Å for and Cx43 [94]. Yet, comparisons between these samples and proteolytically treated Cx32 [95] or Cx43 [96] gap junctions, where most of the C-terminus is removed, yielded no measurable differences in the crystallographically averaged channel structure, indicating that these domains contributed little to the Bragg diffraction data.

3. Current, multidimensional structural analyses

3.1. Recent 3D structures from electron microscopy: going from quaternary structure to secondary structure

A large step towards visualizing the secondary structure of the gap junction was the work of Unger et al. [29,97] (Fig. 1F). This gap junction structure was obtained from preparations of a recombinant Cx43 truncated at Lys 263 (this mutant is denoted as α_1-Cx263T; for comparison, the full-length Cx43 has 382 residues) and expressed in Baby Hamster Kidney (BHK) cells [98]. The effect of reducing the length of the CT was to produce much better quality crystals for in situ crystallization. The resolution of this 3D structure is ~7 Å in the membrane plane and ~21 Å in the perpendicular direction. The outer diameter of the connexon was ~70Å narrowing at the extracellular domains to a diameter of ~50 Å, creating a "waist" in the appearance of the intercellular channel. The channel pore narrows from an apparent ~40 Å diameter at the cytoplasmic opening to ~15 Å at the extracellular side of the bilayer before widening to ~25 Å in the extracellular region. However, it is expected that the diameters should be 10 Å less due to the contributions of the side chains that were not resolved at 7 Å resolution. The narrowest part of the channel would be only 5 Å in diameter. Cx43 channels are permeable to molecules of at least 15 Å. The smaller diameter of the gap junction pore may be due in part to the in the continuous presence of the Cx43 uncoupler oleamide [99]. The thickness of the transmembrane and extracellular domains of the α_1-Cx263T mutant 3D structure is ~150 Å. Strands of mass density extend above the estimated lipid bilayer boundary but cannot be assigned to a particular cytoplasmic sequence. Recently, comparisons of the ~7 Å resolution structures of full-length and trypsinized Cx43 both expressed in BHK cells showed conservation in the 24 transmembrane helices within each connexon and the belt of density in the extracellular vestibule [100]. However, there was no cytoplasmic density in the 3D structure of full-length Cx43 that could be ascribed to the ~13 kDa carboxy tail, suggesting that this regulatory domain has conformational flexibility at neutral pH (Cheng and Yeager, personal communication). Difference projection density maps between full-length and trypsinized Cx43 displayed small positive difference peaks at radius of ~17 Å and small negative difference peaks at ~25 Å radius, indicating that removal of the carboxy-tail elicited small structural rearrangements presumably in the transmembrane helices [100].

The initial projection map contained a ring of transmembrane α-helices lining the aqueous pore and a second ring of α-helices in close contact with the membrane [29]. This projection map suggested that there was a 30° rotation between apposing connexin subunits, confirming the hypothesis made by Hoh et al. [101] that the connexons need to rotate and interdigitate to form a closed seal at the extracellular surface. The subsequent 3-D reconstruction of this map [29] provides the first experimental confirmation of the original topology models predicting a four-helix bundle in the transmembrane domain of each connexin. Twenty-four helical rods are seen in each hemichannel, but the inability to resolve their cytoplasmic or extracellular connections did not allow assignments of helices to specific transmembrane domains (TM1–TM4) in the connexin

structure. The α-helices pack in a left-handed bundle within each connexin subunit, but a single right-handed packing interaction is observed for one of the two possible helix pairs that line the aqueous pore. One of these helices is also one of two helices that are strongly tilted, as originally predicted by the X-ray analysis of Tibbitts et al. [87]. Tilting of this α-helix causes one of the other helices to form a criss-cross arrangement exposing its cytoplasmic end to the channel. Based on its amphipathic character, M3 had previously been proposed as the logical candidate to line the pore [102,103], but there were no clues from the sequence as to the possible identity of the other helix.

Efforts at determining an unambiguous α-helical packing model based purely on the Unger et al. EM structure [29], amino acid constraints and computational modeling represent a promising direction [104]. There is at least one significantly bent helix in the Unger et al. structure (i.e., helix B [29]), and it is tempting to speculate that this may correspond to TM2 which has a centrally conserved proline that might be expected to induce such a kink [105]. This proline was shown to be important in the voltage gating of the channel [106], and Monte Carlo simulations further suggested that the helix may undergo a change in bend from ~37° to ~20° during gating as the result of a broken H-bond [107]. However, in this study, definitive assignment of TM2 to this bent helix has not been possible due to the limited resolution of the Unger model perpendicular to the membrane that does not allow for tracing or identification of the α-carbon backbone within the transmembrane domains. The molecular identification of these helices required mutagenic and biochemical approaches described below [107–110]. TM3 was hypothesized to be the principal pore lining helix because of its amphipathic nature [111], however, as discussed in Section 4, TM1 has also been reported to be the major pore lining helix [112]. The identification of the other helix as either TM1 or TM2 is still a subject of controversy, and may depend on the state of the channel (i.e., whether it is the open or closed state in the Unger structure and whether mutagenic analyses were assayed in whole or hemichannel conformations).

A new model of the arrangement of the α carbon atoms of the transmembrane a helices has been proposed by Fleishman et al. [30]. This model was based on a three-dimensional map, 5.7 Å in-plane and 19.8 Å perpendicular to the membrane plane that was obtained by data analysis refinement of the original 7Å data of Unger et al. [29]. The four transmembrane segments in the oleamide-treated Cx43 truncation mutant structure corresponding to α helices were traced as canonical α helices and the α carbons were assigned to specific amino acid residues in the protein sequence. The criteria for these assignments were evolutionary conservation of residues, hydrophobicity of the amino acid residues, biochemical and phylogenic data from mutagenesis studies and analysis of naturally occurring disease mutations in Cx32. The amino acid sequence of Cx32 was chosen for modeling based on the wealth of data from patients with naturally occurring CMTX mutations. The assumptions put forth by the authors is that, in these highly conserved domains, the structures of these two isoforms share a common architecture, and that highly or strictly conserved amino acid residues will preferentially pack at helix–helix interfaces. Disruption of these interfaces such as those caused by naturally occurring CMTX mutations will eliminate or severely modify functionality by breaking the helix bundle packing. Using this computational approach, Fleishman et al. [30] suggest that the major pore lining helix is TM3 and the minor pore lining helix is TM1. The TM2 and TM4 helices face the lipid environment with TM2 closely apposed to TM1 and TM4 closely apposed to TM3. The arrangement of the canonical transmembrane α helices is shown in a highly schematized illustration in Fig. 2. However, it is important to point out that this is not a consensus model since there is disagreement with some of the mutagenesis studies described in Section 4 of this review [108,110,112]). Errors in assignment of the helix orientations are within 40° and the helical register could also vary by ~1 turn of a helix due to the decreased vertical resolution. Nonetheless, this model provides a valuable starting point for the future design of structure/function mutagenesis studies.

In the Unger et al. [29] structure, the secondary structure in the extracellular domains is much harder to interpret than in the transmembrane domains. The reconstruction has a double-layered appearance that is consistent with the Foote et al. [33] model for a double β-barrel arrangement that would create two concentric cylinders of protein density (Figs. 1G, 3A). It was proposed that the antiparallel β-strands from the E1 and E2 in each connexin combines with the E1 and E2 β-strands from the eleven other connexins in the whole channel to create two concentric anti-parallel β-barrels (one composed of E1 and one from E2) that make a tight seal necessary for a functional channel [33] (see Fig. 3B).

In another set of papers, the question of how the structure at the extracellular surface can influence docking was addressed [34,91,113,114]. The binding of two apposing connexons must be sufficiently strong to create an insulated channel. The nature of this binding was investigated biochemically by developing a reproducible procedure for splitting isolated rodent liver gap junctions. This utilized a combination of urea, chelating agents, and temperature that typically yielded >75% split junctions [34]. The urea treatment appeared to cause no gross conformational changes in the connexons within the membrane, as the packing and structural details of the split and intact structures did not vary in cryo-EM, and images of both structures diffracted similarly to 14 Å resolution [34]. While urea has previously been thought to break the water structure, recently it has been suggested that one mechanism of urea is to interact more favorably with a protein surface than with water, thereby increasing the solubility of a

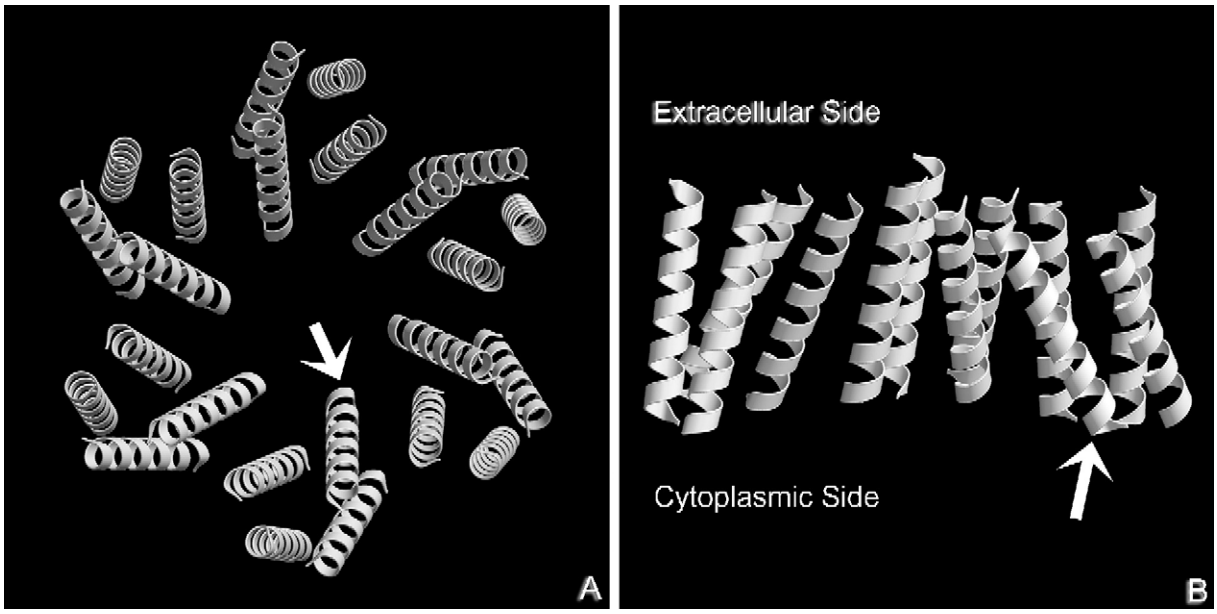

Fig. 2. Spatial arrangement of the transmembrane α helices. Canonical helices were fitted to a 5.7 Å 2D crystal map of the α_1-Cx263T (Cx43 truncated at Lys263) obtained by cryo-EM [30]. This figure was generated using the Protein Data Bank coordinates (file name 1txh.pdb) using the program molscript. (A) View down the cytoplasmic surface of the 6-fold symmetric hemichannel. The arrow indicates one of the six major pore lining helices. (B) Cutaway view of a hemichannel as seen from inside the pore. In this rendering, three of the subunits are visualized in order to view the inside of the pore. As in (A) the arrow indicates one of the three major pore lining helices displayed in this figure.

protein's hydrophobic core, in this case, the surfaces of the lobes of the "undocked" connexon [115]. The reducing agent, dithiothreitol, was not required for splitting the connexon pair [34], consistent with previous demonstrations that the six conserved cysteines in the extracellular loops form exclusively intra-connexin disulfide bonds that are not accessible to external reducing agents [33,116]. It has been proposed that once docking is completed, an exchange of disulfide bonds could stabilize the open conformation. N-glycosylation scanning mutagenesis in which glycosylation sites are artificially introduced at various points in the sequence showed that a considerable fraction of the second extracellular loop is inaccessible [117]. Close inspection of the amino acid sequence for the extracellular loops, E1 and E2, suggests that there are significant stretches of hydrophobic residues. The E1 loop in Cx32 contains 12 hydrophobic residues out of 35 while 21 out of 43 amino acids in the E2 loop are hydrophobic, including a stretch of 11 consecutive hydrophobic amino acids, which is remarkable given that it is localized to the aqueous "gap" region. Hence, hydrophobic interactions are also likely to play a significant role in the stabilizing interactions of these domains.

While calcium ions have been implicated as one of the stimuli for closing the channel, it has been hypothesized that calcium may act in a structural role at the extracellular surface. Opening of hemichannels by low calcium could allow for transport of ATP, glutamate or other signaling molecules or metabolites. It has been speculated that, since EGTA specifically chelates Ca^{2+}, its requirement for gap junction splitting suggests that the binding of Ca^{2+} contributes significantly to interactions that stabilize the docking of apposing connexins [34]. Connexins contain three aspartic acids and three glutamic acids that are strictly conserved in the extracellular loops [118], which represent a possible binding site for Ca^{2+}. In a more recent study, two aspartic acid residues in the E2 sequence of human Cx32 were each mutated [119] and the result in either case was a reduction in calcium-induced closure in these mutant hemichannels when expressed in *Xenopus* oocytes. Functional heteromeric combinations of the two mutated Cx32 forms when expressed in oocytes resulted in the rescue of Ca^{2+} induced blockage. One of these aspartic residues is at a site where the charge is strictly conserved among connexins while the second position is more variable. Gomez-Hernandez et al. [119] proposed that for hCx32 and other isoforms, which contain negatively charged residues at these sites flanking the first and third cysteine residues in E2, a ring of 12 negative charges can form a maximum of 6 binding sites for Ca^{2+}. These sites would mediate both pore occlusion and voltage-gated blocking by physically occluding the opening at the cytoplasmic side. For connexins lacking one of these two charged residues, an alternative binding mechanism would need to exist.

Some evidence that ionic interactions between the extracellular loops could stabilize inter-connexin interactions within a connexon was provided from naturally occurring mutations associated with nonsyndromic hereditary deafness in Cx26 [48]. Neutralization or reversal of the positive charge at R75 in E1 (to W or D, respectively) caused the connexons to dissociate when solubilized in dodecyl maltoside. Connexons composed of wild type or

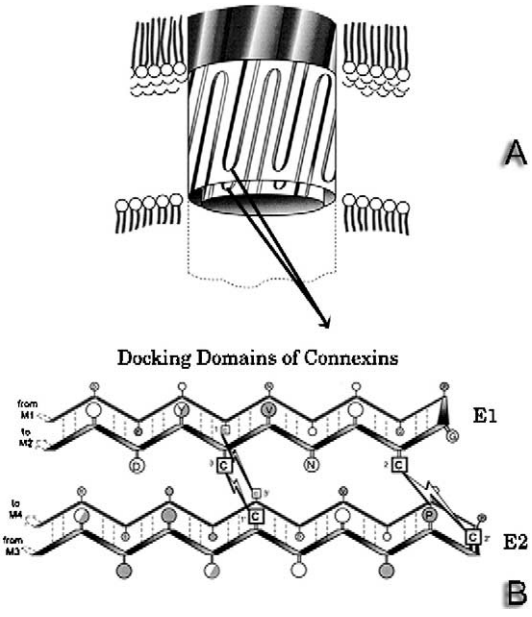

Fig. 3. Proposed arrangement of the secondary structure and disulfide bonds in the extracellular loops. (A) Topology model of the interdigitation of the loops of individual connexins to form a barrel extension at the docking interface between hemichannels. Concentric barrels would be held together by disulfide bonds and would extend from the connexin subunits within the membrane into the extracellular space separating the cells. Two loops are indicated by the arrow pointing to the hypothesized β secondary structure shown in (B). The loops have been shown with an arbitrary tilt to the perpendicular axis of the barrel, consistent with other known barrel structures. (B) From an analysis of rescue of function, cysteine movement experiments, a model is proposed where E1 and E2 form stacked, antiparallel sheets connected by three disulfide bonds. Conserved residues are indicated based on alignments of all vertebrate connexins. Filled circles indicate hydrophobic character, and open circles indicate hydrophilic character. Half-filled circles indicate that either no consensus of hydrophilic or hydrophobic residues exists at this location, or the conserved residue at that location has an amphipathic character. Specific residues are only indicated when at least 14 of the 17 aligned sequences were identical at that position. (Adapted from Ref. [33]).

heteromeric mixtures of mutant and wild type subunits maintained their connexon appearance upon detergent solubilization. The interpretation presented was that R75 serves to stabilize the connexon via intra-connexon associations, possibly salt bridges. The only complication to this model is that another neutralizing mutation, R75A, retained its detergent resistance.

A cryo-negative stain, three-dimensional reconstruction to ~18 Å of rat liver gap junctions [91] revealed six protrusions rising above the membrane on the extracellular side, demonstrating that the contact surface between connexons in apposing membranes is not flat. Connexon docking employing the electron crystallographic hemichannel as input [114] was used to fit the peaks on the extracellular surface of one connexon into the valleys of the opposed connexon generated by a 180° rotation (see Fig. 1I). This fit was optimal when the angle between the peaks of the extracellular surfaces was 30°, agreeing with the conclusions of Hoh et al. [101] and Unger et al. [29]. The docked structure fits into the envelope of the intact gap junction map and the shape tapers like an hourglass towards the middle of the docked hemichannels, a structure that shares the general features of the more detailed 7Å structure [29]. This docking model is also in agreement with expectations from the β-barrel model proposed in [33].

These cryo-EM reconstructions also reveal a flatter cytoplasmic surface, although slight modulations were seen which were distinctly different from the classic skewed-lobe appearance. There also appears to be some stain-excluding mass at the 3-fold axis of the unit cell on the cytoplasmic surface. This was first seen in projection in [61,64] but is absent in other published reconstructions, and likely arose from the cytoplasmic loops, or base of the carboxy tail from each of the six connexin molecules. Another common feature was the tapering of the molecular envelope from the cytoplasmic end to the extracellular end when viewed parallel to the membrane plane. The connexon channel opening measured ~16 Å at the extracellular surface and ~25 Å at the cytoplasmic end, consistent with the 7Å resolution structure. However, it is also important to remember that the uranyl acetate used to contrast the connexon will enhance the appearance of the pore [64] because of its higher negative charge.

3.2. Atomic force microscopy of gap junction channels and hemichannels: flexibility and dynamics studied at molecular resolution

Atomic force microscopy (AFM) [120] provided the first insight into the connexon extracellular surface structure of rat liver gap junctions, containing primarily Cx32 [101,121]. In AFM, the probe tip scans across the surface of the specimens, producing topographs of the surface structures, in contrast to EM, where the images are 2D projections of the 3D object. Sample preparation and imaging procedures of the AFM have been steadily improving, allowing surface structures of native proteins to be observed at a vertical resolution of 1 Å and a lateral resolution of <10 Å [122,123]. AFMs equipped with aqueous specimen chambers reveal biological objects in buffer solution, at ambient temperatures and with outstanding signal-to-noise ratio, allowing observation of conformational changes in single proteins or macromolecular complexes in their native environment under non-destructive conditions [124,125] unlike those in EM. In addition, since the z-modulation in AFM images is very well determined [120,126], thickness measurements on biological specimens can exhibit a precision of a few Å [127], providing accurate measurements for the dimensions of molecular features such as the height of the cytoplasmic and extracellular domains protruding from the lipid bilayer.

In initial studies, it was found that the tip of the AFM cantilever could be used to strip off one of the two bilayers in gap junctions isolated from rat liver, a procedure that the authors titled “force dissection” [128]. The forces necessary

for force dissection are at least ten times larger than the forces used for imaging surfaces (e.g., ~50 versus ~500 pN). The images of the extracellular face revealed the hexagonal subunit structure while the cytoplasmic surface appeared fuzzy and indistinct. In a follow-up study [101], more detailed images of the extracellular surface of force-dissected liver gap junctions showed that connexons in the best images indicated surface modulations that were interpreted as structural protrusions. These images suggested that two apposing connexons fit into one another in an interdigitating arrangement and provided the enticement for pursing the 3D reconstruction of the hemichannel from chemically split gap junctions [91,114].

A recent AFM study showed high resolution images of both the cytoplasmic and extracellular domains [93] using normal and force dissection imaging (Fig. 1D and H, respectively). The images of the extracellular surface are extraordinary in that individual ~15 Å diameter subunits are resolved in the "raw" image. This surface modulation is skewed with respect to the lattice axes and further supports a model for interdigitation of apposing connexons to make the dodecamer [114]. The six subunits, protruding by ~16 Å above the lipid bilayer, were arranged into a donut shaped structure surrounding a central pore. The pores exhibited an average outer diameter of ~49 Å and an average inner diameter of ~15 Å. The correlation average of the connexon showed the structural arrangement of the extracellular domains surrounding the transmembrane pore more clearly. As judged from a standard deviation map, the region of highest variance in the extracellular surface was the central pore, suggesting that some heterogeneous pore diameters may still be found even on this long time scale.

The structural details of the gap junction membrane channels in these images are clearer than previous studies [101,129,130], not only because of the improved technology, but also because of the reduced amount of protein at the cytoplasmic surface compared to Cx32 and Cx43 [130]. Cytoplasmic domains represent ~33% of the amino acids in Cx26, in contrast to ~47% for Cx32 and ~61% for Cx43. The cytoplasmic domains are so flexible that these can be easily moved with the AFM tip. Imaged at higher resolution and an applied force of ~50 pN, the cytoplasmic gap junction surface exhibited donut-shaped structures assembled into a hexagonal lattice with a unit cell distance of ~77 Å. The pores showed an outer diameter ~56 Å and had an inner diameter of ~28 Å. On average, the cytoplasmic domains protruded by ~17 Å from the lipid bilayer. When imaged at slightly enhanced forces of ~70 pN, the cytoplasmic domains were observed to collapse reversibly onto the membrane surface. This collapse of the cytoplasmic domains formed a supra-structure on the membrane surface that reduced the gap junction height by 15 Å, so that the surface structures protruded only ~2 Å above the lipid bilayer. The cytoplasmic domains of this conformation formed an enlarged channel entrance exhibiting an inner diameter of ~47 Å and an outer diameter of ~58 Å. The depth of the pore was about ~16 Å. This flexibility at the cytoplasmic surface is consistent with the model that propose an interaction with the channel pore entrance and the N-terminus or the proposed "ball and chain" mechanism for gating through interactions between the channel pore entrance and the cytoplasmic loop and C-terminus, [131–134].

Large fluxes in cytoplasmic calcium ion concentration have long been postulated as a cellular apoptotic mechanism that uncouples the gap junctions in dying cells, thereby insulating them from healthy neighbors. Calcium-mediated uncoupling has been studied since the 1960s, however, we still do not yet understand the cause and mechanism of channel closure or how this fits into a bigger picture, whereby most cell types, for example astrocytes and HeLa cells, exhibit calcium waves that are transmitted from cell to cell. In addition, as more data are recorded on hemichannels, it becomes clearer that these may exhibit a different gating responses to Ca^{2+} [135,136]. AFM imaging is an excellent method to visualize conformational changes of molecules because the same molecules can be examined under different buffer conditions. In the topographs presented in Müller et al. [93], the extracellular entrance of the pore in Cx26 hemichannels significantly decreased its diameter from ~15 Å to ~6 Å with the addition of 0.5 mM Ca^{2+} (as shown in Fig. 4A and B, respectively). This conformational change was fully reversible and could be repeated over several times over a couple of hours. Connexons with intermediate pore sizes between these two states were also observed. As visualized by the SD map, the extracellular channel entrance represented the most flexible structural region of the connexon surface. The difference image calculated between the $-Ca^{2+}$ and $+Ca^{2+}$ as well as the superposition of contour maps show that the area of highest difference occurs in the pore area, with only slight differences in the subunit topology. Up to a concentration of 2 mM, Mg^{2+} did not influence the appearance of the connexon pore, showing that this conformational change is specific for Ca^{2+}.

A different effect was seen when gap junction plaques were exposed to higher levels of Ca^{2+}. The cytoplasmic surface appeared mottled and maximum thickness of the gap junction plaque increased from ~174 Å to ~180 Å. Material was segregated into microdomains within the plaque producing an increased plaque thickness from 174Å to 180Å and an enhanced surface roughness that prevented resolving whole channels at the cytoplasmic surface by AFM. The significance of these changes was not clear as they were not reversible, although it has been postulated that these two conformational changes could correlate with distinct Ca^{2+} gating mechanisms for hemichannels and whole channels [75].

A new and complementary study on reconstituted Cx43 hemichannels has shown a similar Ca^{2+} effect [137]. In this study, wild type Cx43 hemichannels were isolated from membrane preparations, solubilized with octylglucoside,

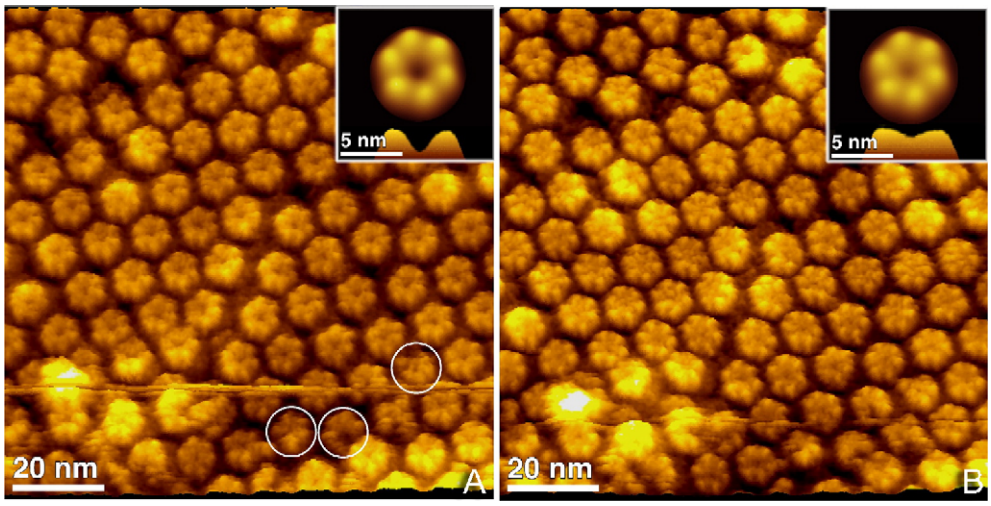

Fig. 4. Conformational changes in Cx26 hemichannels observed in high and low calcium buffers by AFM. (A) AFM topograph showing extracellular connexon surface recorded in a Ca^{2+}-free buffer solution. Individual connexons exhibit defects in the number of subunits, as indicated by the circles. The insets in the top right hand corner show the correlation average of the raw data as well as the profile of the extracellular channel opening (profile at the bottom of the inset). (B) Same connexon surface as imaged in (A), but in the presence of 0.5 mM $CaCl_2$. As visible in the raw data, individual connexons nearly closed their channel entrance. The channel diameter has changed significantly as seen in the correlation averaged top view (inset) and the profile at the bottom of the inset. Superposition of correlation average allows assigning the channel entrance to be the most rigid structural element of the extracellular surface. All images were displayed as relief tilted by 5°. Adapted from Ref. [93].

affinity purified, reconstituted into lipid vesicles and heat induced to form planar membranes. Presumably, these hemichannels would be a mixture of pre-docked or un-docked connexons. Extracellular and cytoplasmic surfaces were identified by the large height differences in the membrane exposed domains and by labeling with antibodies specific to the carboxy terminus. Increasing concentrations of Ca^{2+} caused a reduction in the pore diameter at the extracellular surface in a population dependent rather than a dose-dependent manner, implying that the Ca^{2+} induced closure is an all or none effect. Cations such as Mg^{2+} or Ni^{2+} had no effect, again demonstrating that this divalent induced closure is specific to Ca^{2+}. The pore sizes in the open and closed state in this new study were larger than reported in Müller et al. [93], although this may be due to a difference between the two isoforms or in specimen preparation. From results obtained analyzing AFM interfacial energy maps, Thimm et al. [137] propose the theory that conformational changes occur in the extracellular loops where they are in a more relaxed and flexible conformation in these isolated connexons than in densely packed or crystalline hemichannels or intact intercellular channels.

3.3. Surface plasmon resonance of connexin peptides: probing dynamic structural interactions

The combination of surface plasmon resonance (SPR) and NMR has proven powerful in determining structural interactions between two peptide components [138]. SPR provides accurate estimates of kinetic parameters of intermolecular interactions, while multidimensional NMR provides information on secondary structure conformation. SPR is an optical technique that is used routinely in solid state physics, biosensor, pharmaceutical and analytical chemistry fields to probe structural and molecular interactions, and has been lately applied to interactions of membrane proteins with other molecules as a way of testing for binding partners or ligands [139].

The technique involves the attachment of a probe molecule or peptide covalently linked to a gold-film surface at the bottom of a SPR cuvette and changing the buffer solution with different test compounds or molecules. Light is shone through a prism into the bottom of the cuvette and binding and kinetic changes are detected as alterations in the angle of light reflected from the gold film surface. Positive interactions will result in a plot where the angle of incidence at each resonance frequency versus time is altered from its original spectra. A lack of interactions will appear as a flat line in the response versus time curve [140]. For example, anti-peptide antibodies against an expressed Cx43 CT will elicit a positive response when a Cx43 CT peptide is immobilized on the cuvette. However, anti-peptide antibodies against the Cx43 CL or Cx32 CT showed no binding response.

Relevant to this review on the structure of gap junction proteins, SPR was used in combination with NMR and enzyme-linked absorbent assays to reveal that conformational changes in a complex of CT and CL peptides [133] occur as the buffer solution becomes acidified. An SPR analysis of six peptides from the cytoplasmic domains (NT, CL and CT) showed that only one, corresponding to amino acids 119–144 in the 2nd half of the CL (Cx43L2), bound to the immobilized Cx43CT peptide. This peptide bound in a pH-dependent manner in which binding occurred at pH 6.5, but not at pH 7.4. Subsequent NMR structure determination of the low pH form showed ordered

secondary structure in the Cx43L2 peptide and induced structure in a domain of the CT (see next section). This study emphasizes the dynamic nature of the cytoplasmic domains and that two of the three major topology segments, CL and CT, are not independent sub-domains, but may interact in a coordinated way under physiological stimuli such as low pH gating. Similar conclusions have been reached in early topological analyses of Cx26 in isolated liver gap junctions where antibody access to the CT of Cx26 was only possible after proteolytic cleavage of the CL [77].

3.4. NMR studies of connexin peptides: obtaining structural information for disordered cytoplasmic domains

Because of specimen preparation considerations described above, and size limits for NMR structure determination, NMR studies have focused on a piece-wise approach to understanding the structure and dynamics of aqueous portions of the cytoplasm domains. While the caveat always remains that small synthetic peptides in a non-native environment, and/or without other binding partners, may not reflect the in situ structure, studies have shown that this is a valuable approach for understanding difficult structural problems [141–143] as well as for designing mimetics for ligand-receptor binding. These solution structures also provide insight into the dynamics and flexibility that may occur in the intact connexin.

The first of these studies was the NMR structure determination of a 15-amino acid synthetic peptide corresponding to the sequence of the N terminus of Cx26 (amino acid sequence MDWGTLQSILGGVNK). The solution structure revealed that the first 10 residues contained an α helical conformation [131]. The remaining four residues (12–15) formed an open turn that would allow the N-terminus to bend back and contribute to the cytoplasmic mouth of the pore (see Fig. 1B), as suggested by mutagenesis studies described below (e.g., Ref. [144]). Site directed mutagenesis of G12 (a conserved glycine hypothesized to permit flexibility between the two short stretches of alpha helices) to proline did not disturb the channel function, presumably because the "hinge" structure was still maintained. Other substitutions such as serine, tyrosine or valine, which might be expected to disrupt the turn structure, failed to produce functional channels. Thus, both structure and mutagenesis data converge to suggest that the N-terminus forms a shepherd's hook structure that contributes to the cytoplasmic entrance of the channel. Consistent with this are the observations that additions to the N terminus of tags for live cell imaging such as GFP [81] or a tetracysteine domain tag (G. Gaietta et al., unpublished results) form gap junctions that at low resolution appear normal, but are non-functional, while connexin constructs containing fluorescent tags on the C-terminus are functional [81,145,146]. These results support a hypothesis that the size of these tags interfere with the placement of the N-terminus within the channel rather than changes in specific amino acid interactions between the N-terminus and the pore lining helices. More recently, Oh et al. [147] have shown that the charged residues at the 2nd, 5th and 8th positions in the connexin sequence are important in determining the gating polarity. However, these amino acids contribute to an electric field determined not only by the amino acids in the N-terminus, but also by the major pore lining helix.

As described above, the structure of a peptide consisting of the amino acid sequence of the second half of the cytoplasmic loop of Cx43 became more ordered upon acidification [133] to produce short stretches of α helical conformation connected by a random coil (see Figs. 1C and 5A, C, E). These two α helices are ~7 amino acids long (residues 122–129 and 136–143), and each contains a histidine residue (His126 and His142) that may be protonated at pH 6.5 and could then interact with negative charges on nearby amino acids. The structure of the CT domain (amino acids 254–382, Fig. 1E) that serves as the Cx43L2 binding partner shows one α helix at segment A311–S325 and possibly another at D339–K345. Only slight changes are seen with acidification, resulting in a slight decrease in α-helicity at the N-terminus and an increase at the C-terminus of the peptide [148,149] (Fig. 5B, D, F) although there is a dimerization of the C-terminal peptide seen at low pH. The low pH dimerization of the C-terminal peptide is hypothesized to create a "particle" that now can bind to the cytoplasmic loop that acts as a "ligand" and effects closure of the channel. The NMR solution structure of the S255-I382 peptide shown in Figs. 1E and 5B is consistent with the theme of two short α helices connected by flexible random coil [150].

What is clear from these NMR solution structures is that there is a pattern within the cytoplasmic domains of short (10–12 or less) amino acid sequences that form possibly transient α helices that are connected by longer, highly flexible loops of random coil. There is no evidence for any β sheet in the cytoplasmic domains that would impart a more rigid conformation. This inherent flexibility is important so that, when gating stimuli occur, these domains can re-organize small stretches of amino acids into organized secondary structures that may serve to create inter-connexin or inter-domain interactions [151]. In fact, it appears that, at least at more acidic pHs, the C-terminal domain forms stable dimers [149]. Whether these structures are representative of the connexin in vivo remains to be investigated, but these flexible structures are consistent with EM images of gap junction cross-sections [63,94] and AFM topographs [42,93,101].

4. Linking structure to function: mutagenic, biochemical and physiological strategies

Although the summary of the field in the above three sections illustrates how far we have come in our under-

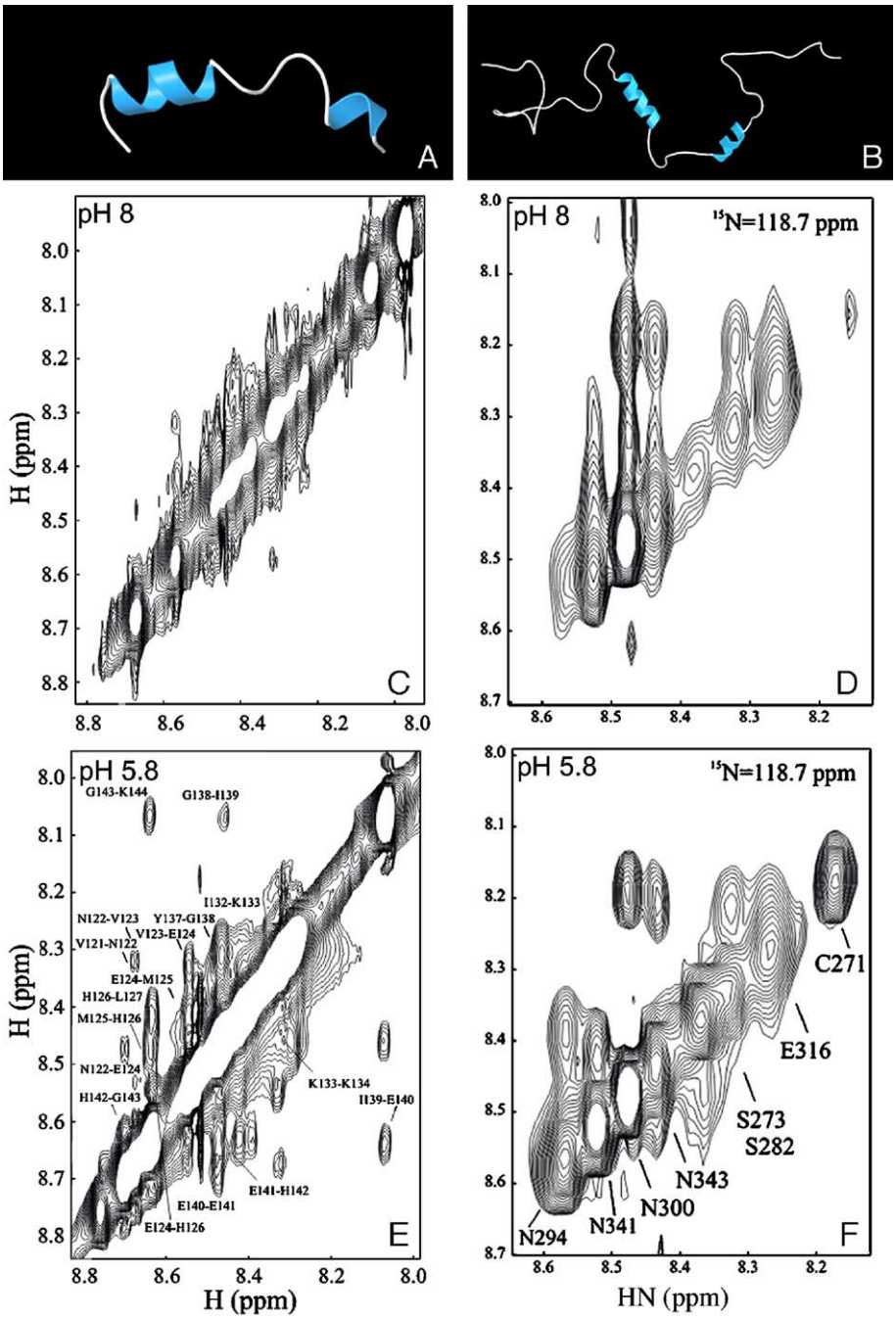

Fig. 5. Conformational differences in the Cx43 cytoplasmic loop (L2) and CT peptides due to pH as measured by NMR. Shown here are the secondary structures of the cytoplasmic (A) L2 peptide and (B) CT peptide at pH 5.8. (C and E) represent the 2D NOESY NMR spectra for the L2 peptide at pH 8 and 5.8, respectively while (D and F) are 3D NOESY spectra for the CT peptide at these same pHs. The spectra displayed for the CT is generated by taking one ^{15}N plane (at 118.7 ppm) from the 3D NOESY spectra. Note the increase in the off diagonal peaks indicating an increase in ordered secondary structure at low pH, particularly for the L2 peptide. Cx43 sequence assignments are indicated on the more ordered pH 5.8 spectra (E and F). (NMR data courtesy of Dr. Paul Sorgen).

standing of gap junction structure since their first definitive morphological identification 38 years ago, the last phase of progress in this long road has been hampered by the difficulty in obtaining direct atomic resolution models of the gap junction channel, a step that will likely require 3-D crystallization of connexins. Nonetheless, in the absence of an atomic structure, a number of mutagenic strategies linked to various biochemical and functional assays have greatly helped to constrain models of gap junction structure and function, as well as help in the interpretation of the structures presented above. In this section, we will summarize the major conclusions or controversies that have arisen from these more indirect structural approaches and how they provide insights into the amino acid arrangements of the pore, its gating mechanisms and structural determinants of selective interactions between

connexin family members. These approaches have also been instrumental, not only in defining the function of gap junctions beyond their role as intercellular channels, but also by identifying an array of molecules that interact with the cytoplasmic domains of connexins to establish a "nexus" for signaling.

4.1. Physiological and mutagenesis studies investigating pore structure

4.1.1. Evidence for selectivity among different isoforms

Although historically gap junctions have been portrayed as non-specific intercellular pores, this view is belied by the diversity within the connexins family, the phenotypes caused by their ablation in mice, and the variety of human diseases linked to connexin mutations. The idea that channels composed of different connexin isoform exhibit characteristic selectivities for ions and small molecules has been emerging over the last decade. Initially, several studies by Veenstra et al. [76,152] demonstrated that channels composed of different connexins showed distinct ion selectivities, ranging from a 10:1 cationic preference (Cx45) to a modest anionic preference (Cx32). In general, cation permeabilities correlate with their aqueous mobilities, but anionic permeabilities suggest that they may interact with simultaneously mobile cations within the aqueous environment of the pore [153]. The modest ionic preferences of connexins have also been associated with rectifying behavior of both hemichannels (e.g. Cx46—[154]) and heterotypic gap junction channels (e.g. Cx32/Cx26—[155]). In early permeability studies on gap junctions of unknown composition at the time, it was proposed that the pore contains a fixed negative charge based on the observation that cations permeate the channels freely, whereas anionic ones are largely excluded [156]. This could also be consistent with the observed preferential binding of cationic negative stains, such as uranyl acetate, in the gap junction pore [64]. More recent electrophysiological analyses have suggested that, in some connexins, charges at the cytoplasmic [157] and extracellular ends [154] of the pore may contribute most significantly to ionic selectivity.

In terms of larger permeants, many comparisons of fluorescent dye transfer and other visually detectable molecules (e.g. neurobiotin) have been performed, although most of these studies did not allow for direct comparisons of single channel permeabilities, percentage of open versus closed channels, or control for the properties of the permeants such that the basis of any observed selectivity could be determined. In some studies, the differences in dye permeabilities did seem to be significantly dependent on charge [74], but in others, it was evident that different features of the permeants must provide the basis for the selectivity displayed by the gap junction channels [158]. This discrimination is often referred to as "permselectivity" and is a separate phenomenon from ion selectivity exhibited by classic ion channels such as the K^+ or Na^+ channel families. Size is clearly one factor in the discrimination by different connexins. This has been documented with permeabilities to anionic fluorescent dyes that show size cut-offs from ~11 to over 14Å depending on the connexin composition of the channels [159,160]. The general consensus from these studies is that Cx43 and Cx32 form the largest functional pore size, Cx26, 40 and 45 form smaller pores, and Cx37 appears the most restrictive, although the precise order is dependent on the sets of probes used, indicative of factors other than size playing a role.

In two studies, neutral permeants have been used and led to conclusions that are quite consistent with those above. Helical oligomaltosides of differing diameters indicated that the presence of Cx26 combined with Cx32 in hemichannels reconstituted into liposomes from isolated liver fractions caused a reduction in functional pore diameter from homomeric Cx32 hemichannels [73]. In a separate study, comparing intercellular gap junctions composed of three different connexins [161], ethylene glycols of increasing size were intracellularly perfused and tested for their ability to enter the channels and inhibit ion flux, a system that had been introduced earlier in the analysis of permeability changes associated with a disease-causing mutation in Cx32 [109]. In decreasing order, the exclusion limits of the channels (proportional to the functional pore diameter) were Cx32 (~12Å)>Cx26 (~10Å)>Cx37 (~8Å). While the absolute size estimates vary, the rank order of connexins sizes estimated from these studies remains remarkably robust. It is worth pointing out we use the term "functional pore size" since the physical pore diameter as measured from EM, X-ray diffraction or AFM may over-estimate the molecular exclusion size.

While the differential permeabilities to these synthetic probes have been instructive, the ultimate interest is to understand the selectivity properties of these channels to natural permeants. It had previously been shown that cAMP [162,163], nucleotides [5,6,164], IP_3 and Ca^{2+} [4,165,166], and metabolites like glucose [167] and amino acids [168] can pass through gap junctions. More recently, a few labs have tried innovative ways to compare the transfer rates of natural metabolites through connexins of defined composition. In a direct capture assay developed by Goldberg et al. [5,169], the metabolite pool of a donor cell population is labeled and the transfer of selected molecules to a recipient population through exogenously expressed connexin channels is monitored by analysis of the contents of the recipient cells after separation from the donors. These analyses reveal differences of over 100-fold in the rate of transfer of ATP through Cx43 and Cx32 channels, despite the similar permeabilities of these channels for anionic dyes like calcein. Other metabolites (glutamate, glutathione, ADP, AMP) also show selectivity, although at lower levels, while adenosine passes preferentially through Cx32 channels.

Consistent with this, a less dramatic, but significant (i.e., 5-fold) difference in permeability for cAMP, introduced

into one cell through open Cx46 hemichannels, was determined through an indirect "reporter system" based on Cl^- influx (and subsequent hyperpolarization of the adjacent cell) through cAMP-gated CFTR channels, showing Cx43 > Cx32 ~ Cx45 [170]. An analogous reporter system was also developed for a mammalian cell system using fluorescent techniques. cAMP, released from a caged form in one cell through a focused laser, was observed to pass to an adjacent cell by virtue of its activation of a cyclic nucleotide-gated Ca^{2+} channel that resulted in a change in fluorescence of a Ca^{2+} sensitive dye [171], A reporter system was also recently employed in determining the relative IP_3 permeability of connexin channels [167], and documenting a surprisingly specific loss of IP_3 transfer through a deafness-associated mutation of Cx26 [172]. Clearly, the properties being distinguished by the channels may be quite subtle. Reconstituted hemichannels composed of predominantly Cx32, or a mixture of Cx32 and Cx26, show distinct permeabilities for cGMP, but the similar permeabilities for cAMP [73]. Based on both the size of the gap junction channel, and the permeability properties described above, it seems likely that the molecular mechanism for selectivity in connexins is distinct from that seen in studies of other ion channels, such as the voltage-gated K^+ channel where direct chelation of dehydrated ions is proposed [173]. Indeed, the rate of flux of dyes through gap junction channels has been estimated to be 1–2 orders of magnitude higher than predicted from passive diffusion based on the bulk cytoplasmic concentration of the dyes in each cell, and the single channel conductances of the pores [159,160]. This result indicates that there are likely to be weak affinities between permeants and the pore wall that result in a preferential partitioning of the dyes into the channel, thereby increasing the probability of occupancy in the channel, and thus the effective concentration gradient and flux rate.

4.1.2. Pore architecture and the structural basis for selectivity

Several strategies have been used to identify the amino acids that form pore-lining domain of connexins. The first of these involved the identifying mutations or chimeric constructs that induced a modification of channel properties, with the inference that the modified residue or region must contribute to the pore. A CMTX associated mutation, S26L, in TM1 of Cx32 was found to cause a reduction in the size cut-off of these channels, suggesting a change in effective diameter from 10 to <3Å [109]. Exchange of E1 domains between Cx32 and Cx46 resulted in exchange of the ion selectivities and voltage gating characteristics of these pores [154], while exchange of TM1 from Cx46 with that of a chimera of Cx32/43E1 resulted in shift of gating and single channel conductance properties towards the Cx46 pattern [174]. In contrast to these results implicating TM1 as contributing to the pore lining, mutation of a residue in TM2 (V84L), that is associated with inherited deafness, was found to selectively inhibit passage of IP_3 through gap junction channels, while not affecting either ion or dye (Lucifer yellow) flux [172]. Cytoplasmic domains have also been proposed to influence the pore structure, as mutants in the N-terminal domain [157] and phosphorylation of the C-terminal domain [175] have both been shown to modify single channel conductance (γ_j).

Independent studies targeted at identifying determinants responsible for the opposite gating polarities of Cx32 and 26 identified the first 10 residues of the N-terminus [131,176], particularly the glutamine at position 2 (N2) [144] as playing critical roles, as well as two residues at the beginning of E1 (E41 and S42 in Cx32, see Fig. 2) [144]. The role of the N-terminal domain was further supported by recent findings that implicated E9 and E13 of Cx40 in defining the gating properties of these channels [157], although these same positions do not seem so critical for Cx43. Based on the supposition that residues involved in sensing voltage drops between cells (V_j for transjunctional), as opposed to across the membrane (V_m), should be exposed to the intercellular channel itself [177], the N-terminus and E1 can be inferred to contribute to the pore lining.

A more direct approach to mapping the residues that contribute to the pore, which has proven very useful in other ion channel studies, is the use of thiol reagents to react with cysteines introduced individually for each residue in the transmembrane domains (a techniques referred to as SCAM for Substituted Cysteine Accessibility Method). If exposed to the pore, the cysteine will react with the introduced thiol reagent, resulting in a reduced conductance of the channel. Hemichannels provide the most ready access for introducing the reagents, and several studies have mapped pore lining residues in Cx46 and chimeric Cx32/Cx43E1 hemichannels. All have focused on TM1 and E1, with some analysis of TM3. Initially, two sites in TM1 (I33 and M34 in Cx32, see Fig. 6) were found to be most reactive, while three in TM3 (S138, E146 and M150, see Fig. 6) reacted to a lesser degree [110].

Subsequently, analysis of Cx46 hemichannels in excised patches at the single channel level [112] revealed reactivity at L35 (the equivalent position to M34 in Cx32) and A39 (V38 in Cx32) in TM1, as well as E43 (S32 in Cx32), G46 (G45 in Cx32) and D51 (S50 in Cx32) in the E1 loop. Notably, in the E1 loop, the ion selectivity of the pore was affected predictably by the charge of the thiol reagent or the substituted residue [112]. Although not all TM domains were tested, TM3, which had shown some reactivity in the study by Zhou et al. [110], showed no reaction in this study. However, the overlap in sites tested was small. In addition, while the study by Kronengold et al. [112] employed more sensitive single channel analysis, the reversible MTS reagents employed were significantly smaller than the maleimide variant used by Zhou et al. [110], and may not have caused significant channel block. One caveat to these studies has been that they are restricted to analyses of hemichannels, so that the extent to which the results can be

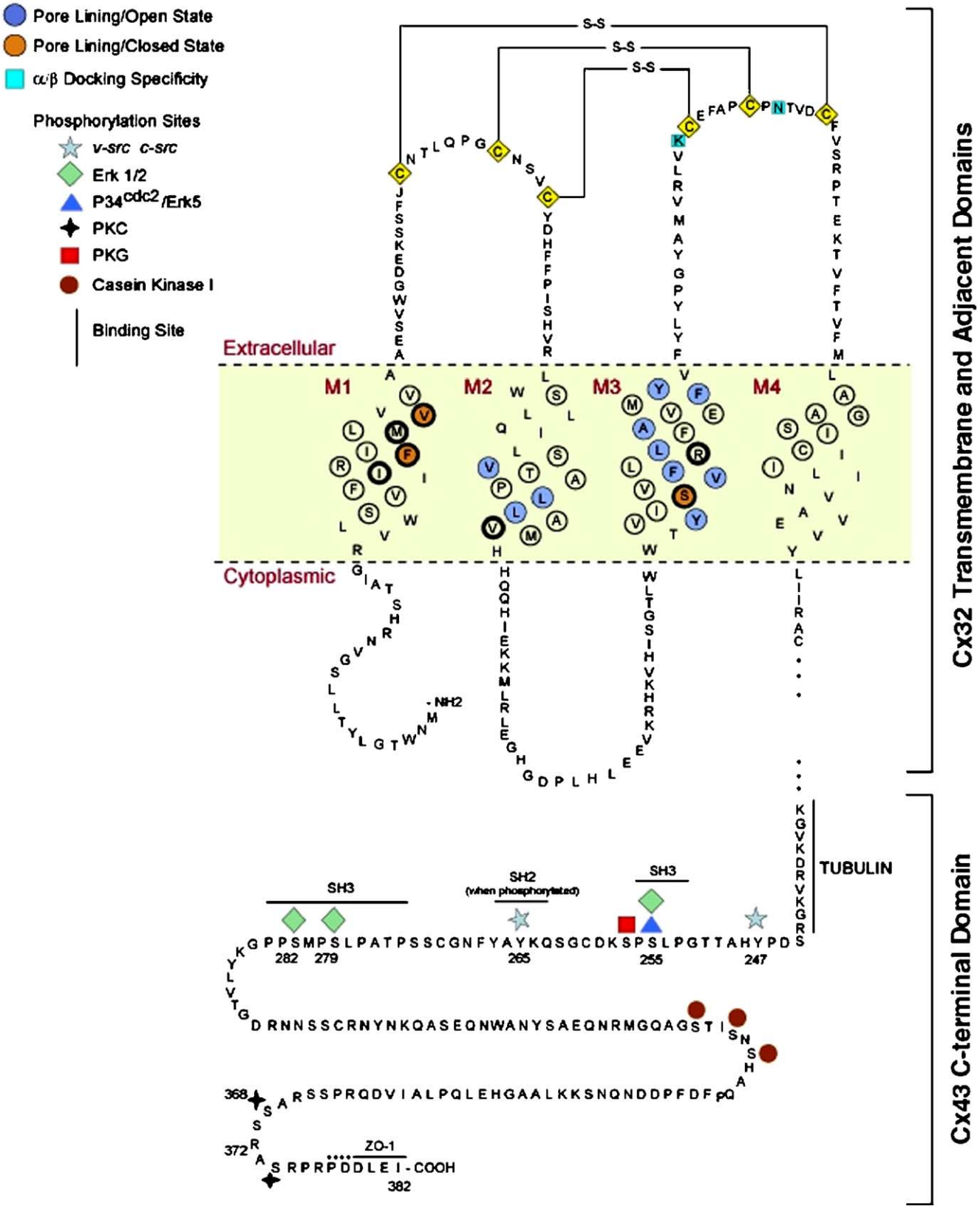

Fig. 6. Composite of amino acid sequences for Cx32 and Cx43 with functionally important residues indicated. This figure contains a summary of mutagenesis studies showing phosphorylation sites, pore lining residues and binding of interacting cytoplasmic proteins. See text for detailed references. Adapted from Ref. [222].

extrapolated to gap junction channels between cells is dependent on the degree to which the pore structure might be modified on docking of hemichannels to form complete intercellular channels.

Extension of the SCAM mapping approach to the full intercellular channel was made possible by the development of a paired oocyte perfusion chamber that allowed access of the thiol reagents through the cytoplasm [108]. A mapping of all 4 TM domains of Cx32 initially revealed reactivity in each domain. However, if sites where the gating characteristics of the channel were modified by the cysteine substitution (stabilizing a closed state of the pore) and sites that could be shown to be accessible by penetration of the thiol reagent into the membrane bilayer from the extracellular surface (and not the pore) were excluded, reactivity was restricted to 7 sites in TM3 and 2–3 at the cytoplasmic end of TM2 (blue circles in Fig. 6). In both cases, reactivity was confined to one face of the helix, although the helical periodicity appears to break down at the extracellular end of the TM3, consistent with a distortion of the main pore lining helix at this point in the Unger et al. structure [29]. Surprisingly, exclusively non-polar residues were found to line the gap junction pore. This suggested a model where TM3 lines the intercellular channel along its full length, with TM2 contributing to the wider cytoplasmic mouth of the pore in the open state. TM1, however, does appear to have significant exposure to the pore in the closed state, but could not be tested in the open state.

The conclusions from SCAM mapping of gap junction channels are quite distinct from the observations described above for hemichannels, where TM1 showed the most reactivity. The resolution of these disparate findings remains, at this point, far form clear, as different thiol reagents and different modes of recording (single channel analysis or macroscopic, based on whole cell, or dual cell voltage clamp) were used, and different connexins examined (Cx32 for gap junction channels and Cx46 or a Cx32/43 chimera for hemichannels). It is also possible, as noted above, that sampling different states of the channel (e.g. hemichannel and gap junction channel) could contribute to the variability in the results. Several studies have shown that hemi-channel and gap junction channel properties for the same connexin are quite similar in terms of gating, single channel conductance and permeability, suggesting similar pore structures. However, this has only been done for connexins that readily form Ca^{2+} regulated hemichannels (i.e., Cx46 [75,178,179] and Cx50 [180,181]).

The patterns of conserved residues between connexins, and locations of disease associated mutations from Cx32 and Cx26, have been used recently to try to model the transmembrane helices to the low resolution helical profiles seen in the 3D EM map [30]. Ultimately, this does not resolve the issue, as much of the SCAM data reported above are used as a basis for initially limiting the parameters of the model. Hence, it is perhaps not surprising that the favored model from this analysis represents a hybrid between different experimental results, proposing TM3 as the main pore lining domain, with TM1 playing a supporting role at the cytoplasmic mouth. Nonetheless, the detail that this model provides regarding possible interactions of residues between helices provides an excellent basis for experimental testing and should catalyze the field to perform the kind of experiments that will ultimately resolve these issues.

Gap junction channels are also unique in that at least one third of the channel lies outside the membrane in the "gap" that separates the cells. This domain is of particular interest for several reasons. Firstly, it is one of the only places in nature where the docking interface between two proteins forms an electrically tight seal that excludes ion exchange between two aqueous compartments without the aid of lipid. Secondly, mutagenesis and substitution studies of E1 [112,154] suggest that this domain may contribute to the ion selectivity of gap junction channels. Thirdly, it is a site where the selectivity of heterotypic interactions between connexins occurs (discussed in 4.3 below). Finally, the docking process between connexin hemichannels appears to also cause channel gating, as hemichannels are predominantly in a closed state on the cell surface. Mutagenic strategies have yielded some insight into the molecular structure of this portion of the pore. Foote et al. [33] showed that moving any of the six conserved cysteines in the two extracellular loops of Cx32 invariably destroyed function of the channels, as had been shown for deletion of the cysteines previously [182]. However, compensatory movement of the appropriate second cysteine was found to rescue function, consistent with intramolecular disulfides between the loops that had been deduced earlier [116]. A comparison of the patterns of movements that effectively reconstituted normal channel function revealed that the first cysteine of each loop connected with the third cysteine of the other loop, with the periodicity of the successful pairings arguing persuasively for a β-sheet structure. This led to the model (Figs. 1G and 3), where the two loops form a stacked β-sheet held rigidly together by disulfides. These stacked β-sheet "fingers" from each hemichannel could then interdigitate to form two concentric 24 stranded anti-parallel β-barrels. Due to the difference in diameters of the concentric barrels, one would expect to see breaks in the outer one. Although this proposed structure was largely a theoretical deduction, the model fits the low resolution structure of the Cx43 gap junction channel published a year later very well [29]. It is also consistent with the rotation and interdigitation of the two hemichannels seen in AFM images [93,101], and deduced from EM structures [91,97,114]. Unfortunately, these studies have provided no information on the residues that line the pore. Evidence derived mostly from hemichannels [112,144,176] indicates that residues in E1 are exposed to the pore and modulate ion selectivity, making it the likely candidate for pore lining in gap junctional channels, but a definitive mapping in this configuration of the channel remains a challenge for the future.

The variable cytoplasmic domains of connexins are also likely to contribute to the mouth of the channel. In particular, the N-terminus of Cx26 has been shown by NMR to form a short α-helix, followed by a bend at residues 12–15 ([131]—Fig. 1B). This structure is consistent with mutagenesis studies on the effects of charge at the N-terminus on the polarity and steepness of voltage gating [144], as well as their effects on single channel conductance [157], which led to a model where the N-termini fold back and contribute to the cytoplasmic mouth of the pore. Other evidence also indicates that the large C-terminal domain of connexins may also contribute to defining channel properties, as truncation of this domain in Cx43 has been shown to modify channel conductance [183], as has phosphorylation events in response to TPA [175,184], possibly at the S368 site that has been mapped as a target of PKC [185] at the very C-terminal end of the tail (Fig. 6).

4.2. Mutagenesis studies of the gating domains

The gating properties of gap junctions are complex, in part due to the in series combination of two channels, but also because these channels respond to a number of stimuli, including voltage (both transjunctional and transmembrane), pH, Ca^{2+} and phosphorylation events. The properties of the gating processes have been well described elsewhere, and here we will only highlight what structural insights have been obtained regarding their mechanisms.

4.2.1. Structural aspects of voltage gating

The responses of gap junction channels and hemichannels to voltage are complex, and generally characterized by slow kinetics (time-constants in the hundred of milliseconds) compared to that seen in ion channels. This has been thoroughly reviewed in an earlier issue of this review series [186] and will not be repeated here, where the focus will be on the identification of domains and residues that contribute to various aspects of the multiple gating responses of gap junctions. It should be noted at the outset, however, that the deduced links of structure to functional states in terms of gating are complicated by overlapping gating mechanisms, and when based on macroscopic recordings alone (rather than including single channel analyses), can be misleading.

Sensitivity to transmembrane voltage (V_m), the typical characteristic seen in most membrane ion channels, is seen infrequently, and only to a modest degree in vertebrate gap junctions composed of connexins [187,188]. However, two charged residues in the C-terminal domain (R243 and D245) of Cx43 have been identified as playing a significant role in the V_m sensitivity of this connexin [188]. In contrast to V_m sensitivity, virtually all gap junctions respond robustly to differences in the voltages of the coupled cells (transjunctional voltage or V_j), although the level of sensitivity, degree of closure, polarity and kinetics vary between connexins. In hemichannels, this voltage gating is manifested as a sensitivity to transmembrane voltage. In this configuration, two types of gating are seen, often with different polarities. In one, which seems most characteristic of the gating seen in gap junctions, the channels close rapidly to a sub-conductance state that can be 15–40% of the fully open state. This is called "fast voltage gating". In the second, the channels close more slowly, but completely, with no residual coupling. This has been referred to as "loop gating" [75], as it closely resembles the currents that have been observed when gap junction channels first form, or disassemble, a process that probably reflects docking of the extracellular loops triggering channel opening [189].

Contrary to the voltage-gated channels, no S4 domain with like charged residues concentrated on one side of a transmembrane domain is found in connexins. However, as summarized above, TM1 and its flanking regions seem to play a central role in voltage sensing, as the N-terminus [131,144] and charged residues at the TM1/E1 boundary [144,176] appear to define both the slope and polarity of the gating response. A model has been proposed involving charges on the N-terminus being drawn into the pore [147], resulting in gating either by direct occlusion, or instigation of a conformational change that ultimately closes the channel.

The latter seems more consistent with the slow time course of gating, and the identification of mutations throughout the transmembrane domains that affect voltage gating. Several residues in TM1, when mutated, have been shown to significantly modify the gating behavior of the channel in Cx32, usually by shifting the voltage response and stabilizing the closed state of the channel (see residues in bold circles in Fig. 6). These residues are generally aligned along one face of the helix, suggesting that this may define an important site of helix–helix interaction involved in voltage gating. This pattern of mutations of residues along one face of a helix causing shifts in the gating response of the channel is also seen in TM2 and TM3 (Bold circles in Fig. 6). TM2 has previously been implicated in voltage gating due to a strictly conserved proline (P87 in Cx32, see Fig. 2) located centrally in this helix. Mutation of this residue (in the case of Cx26 [106]) or adjacent residues in Cx32 (S78, L83 and T86) [107] cause a major change in voltage gating where the closed state is stabilized at rest, and voltage now causes the channel to open. This suggests models where the proline within TM2 induces a bend within the helix that itself promulgates a conformational change from helix to helix [106] or serves as a flexible point where changes in the "kink" of the helix mediate conformational changes that lead to gating [107]. A complication to the interpretation of these results is that mutation in other connexins of the orthologous residues described above for Cx32 frequently has no effect on gating [107]. This would suggest that either helix packing or gating mechanisms vary significantly between connexins, or that the interpretation of the effects of mutagenesis within the membrane is more complex.

The location of the gate itself was investigated in hemichannels and localized within TM1 near M34 [190]. However, in Cx32 intercellular channels, this site was shown to be exposed extracellularly in the closed state of gap junctions, and hence is unlikely to line the pore [108]. Recent SCAM mapping of open and closed states of Cx32 intercellular channels indicates that the channel closes at a defined location towards the extracellular end of TM3, leaving large parts of the pore still accessible to solvent, consistent with the structure deduced from electron crystallography [29]. The apparent discrepancies relating to the mapping of the gate in TM1 of hemichannels and TM3 in gap junction channels could result from inadvertent mapping of conformational changes removed from the pore, or from significant differences in the structures, and gating, of the pore between hemichannels and intercellular channels.

While much of the process of voltage gating appears to occur within the membrane, other parts of the protein may also influence the process. Modifications, such as addition of EGFP to the C terminus [191], or truncation of the C-terminal domain of Cx32, Cx40 or Cx43 [188,192] appear to modify the fast V_j gate of these channels, so that slower, full closure of the pore characteristic of loop gating is observed. The interpretation of these results can be complex, as it could reflect significant changes in a gating mechanism, or shifts in its voltage sensitivity that may unmask other gating events. However, in the latter case, addition of the C-tail domain as a separate peptide, while not rescuing gating fully, did re-establish the presence of a residual conductance state [192], suggesting that fast voltage gating may require interactions between the transmembrane pore and the cytoplasmic C-terminus. This influence of cytoplasmic domains on Vj gating may, however, not be universal to all connexins, as similar modifications of Cx37 have no effect on voltage responses [192].

4.2.2. pH and phosphorylation mediated gating

Acidification of the cytoplasm leads to closure of the gap junction channels composed of most connexin isoforms, although the sensitivity differs. Delmar and colleagues have investigated this process extensively and found that deletion of the C-terminal domain eliminates this response, but that it can be reconstituted by adding this region back as a separate domain [193]. These authors hypothesize that closure occurs in an analogous manner to the "ball and chain" inactivation gate of K^+ and Na^+ channels [194]. The domain within the C-terminal domain likely to be responsible for this has been roughly mapped using deletion mutagenesis [195]. Although there is still some controversy associated with which part of the pore mouth this region interacts with, Ek et al. [196] implicated a His residue at the TM2/Cytoplasmic loop (CL) interface. In contrast, a peptide corresponding to the C-terminal half of the cytoplasmic loop was shown to interact with the C-terminal domain at acidic pH [133], causing conformational changes in both domains [133,149] (see Fig. 5). Wang and Peracchia [197–199] have proposed a slightly different model for Cx32 involving competitive binding between the N-terminal half of CL with either the C-terminal half of CL, or the membrane proximal portion of the C-tail. Finally, in an intriguing series of studies, Bevans and Harris [200] have proposed that pH gating may actually arise from titration and selective binding of endogenous aminosulfonates to connexins. This would explain why some connexins with no significant C-terminal domain remain pH sensitive, and is also consistent with the observation from cytoplasmic perfusion studies that other factors may be required for pH gating [201]. However, it should be noted that Cx46 hemichannels in excised patches appear to display pH sensitivity in the absence of any added cytosolic material [179].

In terms of the regulation of gap junctions in situ, gating of the channels in response to phosphorylation is likely to be far more relevant than any of the processes discussed above. While there are many targets for different kinases on the C-tail of connexins, only a few have been associated with acute gating of the channels. These have been most thoroughly mapped on the primary sequence of Cx43 as shown in Fig. 6. Several sites have been linked to regulating the assembly of gap junctions: S328/330 (Casein kinase [202], S368 Protein Kinase C [203] and residues 251–257 [204]). Disassembly and/or degradation of connexins have also been shown to be regulated by other sites (e.g., a tyrosine sorting signal, Y286 [205]) and kinases, including PKC [206] and p34cdc2 [207], with the latter likely to play a role in the transient uncoupling of cells during mitosis.

Two kinase systems have been associated with direct closure of gap junction channels, notably v-src [208–210] and ERK [134,211], while PKC has been associated with modulation of channel conductance [175]. V-src is known to target Y265 and Y247 on the C-tail of Cx43 [210] and also appears to bind to the tail through a combination of SH3-driven interactions (sites on the C-tail indicated in Fig. 6) and SH2 binding to the phosphorylated tyrosines [212]. Although phosphorylation of tyrosines on, and binding of v-src to, Cx43 have been shown to be necessary for uncoupling in cells chronically expressing v-src, other data in both oocyte and mammalian systems suggest that acute closure of Cx43 channels upon initial expression of the oncogene is dependent on ERK phosphorylation at S255, 279 and 282 [134]. This is likely to work in an analogous way to the transient uncoupling of cells in response to growth factors like EGF and PDGF, as this has also been shown to be dependent on ERK, in addition to other kinases such as PKC [211]. ERK-dependent gating was also shown to be mediated through a "ball and chain" mechanism similar to that of pH gating, but utilizing different sites on the protein. This appears to be true whether the ERK is activated by growth factors (e.g. Insulin like growth factor [213]) or oncogenes, such as v-src [134]. Thus, it is likely that modification of the C-terminus of connexins by a variety of effectors can regulate coupling through acute

gating, or other more long-term mechanisms that could include assembly, or failure of the channels to open on docking (e.g. loss of the "loop" gate).

4.3. Heterologous interactions between connexins

4.3.1. Structural information derived from mutagenesis studies of heterotypic interactions

A unique aspect of gap junction channels is that they are composed of two hemichannels from each cell that must dock in order to complete the intercellular conduit. This docking typically occurs between hemichannels composed of the same connexin, but can also occur between different members of the connexin family (heterotypic coupling). As discussed already, whether heterotypic pairing occurs in situ is still somewhat controversial. Extensive comparisons of compatibility between connexins expressed in exogenous systems have been performed in several labs, with the conclusion that, while there is specificity, there are also many heterotypic combinations that do produce functional channels. Overall, connexins within a homology class [(i.e., α or β-(1))] tend to couple with one another, but inter-class coupling is relatively rare (reviewed in Ref. [214]). However, there are connexins that couple with both α and β groups (e.g. Cx46), some connexins that show high levels of specificity, including one that only couples homotypically (i.e., Cx31), and yet others that seem to show an inverted coupling specificity (Cx50, an α-connexin that couples almost exclusively with β-connexins, and Cx30.3, a β-connexin that couples preferentially with α-connexins). Domain swapping experiments suggested that E2 appeared to be responsible for the selectivity of coupling between Cx50, Cx46 and Cx43 [84]. The observation that "incompatible" connexins (specifically Cx43 and 26) can actually segregate within a plaque, while "compatible" connexins tend to mix [80] certainly suggests that the lateral interactions between channels in large plaques may also play a significant role in the assembly of gap junction plaques.

One interesting aspect of docking is whether the opening of the intercellular channels is obligatorily linked to the docking process. While most mutations either result in problems with assembly, or allow formation of functional channels, often with modified properties, some have been identified that allow structurally identifiable gap junctions to form, but never show functional intercellular coupling. Several of these mutants, associated with a disease phenotype, occur predictably in the extracellular loops. However, more surprisingly, the cytoplasmic end of TM3 is also involved in the linkage between docking and channel opening, as mutation of a conserved threonine here (T135 in Cx26 and T134 32), results in non-functional channels, but does not interfere with the structural assembly of gap junctions [215]. This is consistent with the finding that exchanges of the cytoplasmic loops of Cx43 and 40 can also influence docking specificity of these connexins [85].

4.3.2. Structural information derived from mutagenesis studies of heteromeric interactions

Hemichannels of heterogeneous connexin composition can also form within a cell, adding to the complexity of gap junction channel types that exist in most cells, where the expression of two or more connexins is often seen. The rules governing which connexins interact are less well described for these heteromeric interactions, as they are more difficult to detect. Nonetheless, initial comparisons with a limited number of connexins are consistent with the same tendency to prefer interactions within a homology class. For example, Cx32 and Cx26 (both β-connexins) interact with one another [47,216], but not with the α connexin, Cx43 [217]. Cx43, however, can interact with Cx40 [218], Cx45 [219] and Cx37 [220], all α-connexins. Cx50 and Cx46, also α-connexins, were demonstrated to interact heteromerically using biochemical means in the lens [45], while Cx26 and Cx32 formed heteromeric hemichannels in liver [44]. Deletion studies in a cell-free translation system implicated the N-terminus and TM1 as principal components in the specificity of these interactions [217]. These studies are hard to interpret given that the proteins that were oligomerizing were missing part of their structure, so that non-specific aggregation may have resulted. Subsequently, using a less destructive, site-specific approach, Falk et al. have gone on to identify two sites in the N-terminus (amino acid positions 12 and 13 in Cx43, D12 and K13) and two in TM3 (amino acids positions 152 and 153 in Cx43, L152 and R153) that appear to dictate the specificity of oligomerization between Cx32 and 43 [221]. This is consistent with the observation, using various chimeras, that TM3 was essential for the oligomerization of connexins, although this study did not specifically address the issue of specificity [223].

5. Concluding remarks

In this review, we have surveyed the gap junction literature to provide an up to date depiction of the molecular structure of the gap junction channel. This overview also discusses some of the nuances of the connexin family that relate to an individual member's function that complicate the structural biologist's quest for a universal 3D structure, but are an integral part of the role gap junctions play across an entire organism. In many ways, it is the differences, not the similarities, between the isoforms that make them interesting and compelling subjects of study. While much is known about electrophysiological properties of connexin channels, we still do not know the molecular mechanism by which the gates within the channel open and close, or how this relates to a structure that has both very rigid domains and very flexible regions. While several studies indicate that the gating of hemichannels does reflect gating events seen in the whole channels, this may not be true in all connexins and it would appear that hemichannels may have some unique gating

that is not seen in gap junction channels (e.g., sensitivity to extracellular Ca^{2+}). Perhaps, most importantly, we are still a long way from understanding the molecular basis of the unique selectivity that these channels display. The results of these studies will have bearing not only on connexinopathies, but also on developmental processes where having the correct connexins in place results in proper transmission of regulatory signals. The discovery of connexin diseases has increasingly fueled our investigations towards an atomic model of a canonical connexin that in turn would lead to the design of experiments aimed at understanding connexin differences.

Acknowledgements

We thank Drs. Priscilla Purnick, Terry Dowd, Mario Delmar and Paul Sorgen for the atomic coordinates of their NMR studies used to create the images shown in Figs. 1 and 5 and to Dr. John Badger for generating the molecular graphics shown in Figs. 1, 2 and 5. We are grateful to Drs. Delmar and Sorgen for providing us not only with the atomic coordinates of their C-terminus structure, but also the NMR spectra prior to publication. We are also deeply appreciative of the talents and efforts of Jim Stamos in compiling the montage of images shown in Figs. 1 and 6. This work is funded by NIH grants GM065937 (GES), GM072881 (GES), GM048773 (BJN), CA048049 (BJN), RR04050 (Mark Ellisman) and NSF grant MCB-0131425 (GES).

References

[1] J. Eiberger, J. Degen, A. Romualdi, U. Deutsch, K. Willecke, G. Sohl, Connexin genes in the mouse and human genome, Cell Commun. Adhes. 8 (2001) 163–165.
[2] P. Phelan, T.A. Starich, Innexins get into the gap, Bioessays 23 (2001) 388–396.
[3] Y. Panchin, I. Kelmanson, M. Matz, K. Lukyanov, N. Usman, S. Lukyanov, A ubiquitous family of putative gap junction molecules, Curr. Biol. 10 (2000) R473–R474.
[4] H. Niessen, H. Hart, P. Bedner, K. Krämer, K. Willecke, Selective permeability of different connexin channels to the second messenger iositol 1,4,5-triphosphate, J. Cell Sci. 113 (2000) 1365–1372.
[5] G.S. Goldberg, P.D. Lampe, B.J. Nicholson, Selective transfer of endogenous metabolities through gap junctions composed of different connexins, Nat. Cell Biol. 1 (1999) 457–459.
[6] G.S. Goldberg, P.D. Lampe, D. Sheedy, C.C. Stewart, B.J. Nicholson, C.C.G. Naus, Direct isolation and analysis of endogenous transjunctional ADP from Cx43 transfected C6 glioma cells, J. Cell Sci. 239 (1998) 82–92.
[7] N.B. Gilula, O.R. Reeves, A. Steinbach, Metabolic coupling, ionic coupling, and cell contacts, Nature 235 (1972) 262–265.
[8] D.L. Paul, New functions for gap junctions, Curr. Opin. Cell Biol. 7 (1995) 665–672.
[9] C.R. Green, N.J. Severs, Distribution and role of gap junctions in normal myocardium and human ischaemic heart disease, Histochemistry 99 (1993) 105–120.
[10] M.V. Bennett, R.S. Zukin, Electrical coupling and neuronal synchronization in the mammalian brain, Neuron 41 (2004) 495–511.
[11] P.I. Patel, J.R. Lupski, Charcot–Marie–Tooth disease: a new paradigm for the mechanism of inherited disease, Trends Genet. 10 (1994) 128–133.
[12] S.S. Scherer, L.J. Bone, S.M. Deschênes, A. Abel, R.J. Balice-Gordon, K.H. Fischbeck, The role of the gap junction protein connexin32 in the pathogenesis of X-linked Charcot–Marie–Tooth disease, Novartis Found. Symp. 219 (1999) 175–187.
[13] D.P. Kelsell, J. Dunlop, H.P. Stevens, N.J. Lench, J.N. Liang, G. Parry, R.F. Mueller, I.M. Leigh, Connexin 26 mutations in hereditary non-syndromic sensorineural deafness, Nature 387 (1997) 80–83.
[14] G. Richard, L.E. Smith, R.A. Bailey, R. Itin, D. Hohl, E.H.J. Epstein, J.J. DiGovanna, J.G. Compton, S.J. Bale, Mutations in the human connexin gene GJB3 cause erythrokeratodermia variabilis, Nat. Genet. 20 (1998) 366–369.
[15] D. Mackay, A. Ionides, Z. Kibar, G. Rouleau, V. Berry, A. Moore, A. Shiels, S. Bhattacharya, Connexin46 mutations in autosomal dominant congenital cataract, Am. J. Hum. Genet. 64 (1999) 1357–1364.
[16] A. Shiels, D. Mackay, A. Ionides, V. Berry, A. Moore, S. Bhattacharya, A missense mutation in the human connexin50 gene (GJA8) underlies autosomal dominant "zonular pulverulent" cataract, on chromosome 1q, Am. J. Hum. Genet. 62 (1998) 526–532.
[17] W.A. Paznekas, S.A. Boyadjiev, R.E. Shapiro, O. Daniels, B. Wollnik, C.E. Keegan, J.W. Innis, M.B. Dinulos, C. Christian, M.C. Hannibal, E.W. Jabs, Connexin 43 (GJA1) mutations cause the pleiotropic phenotype of oculodentodigital dysplasia, Am. J. Hum. Genet. 72 (2003) 408–418.
[18] J.-P. Revel, M.J. Karnovsky, Hexagonal array of subunits in intercellular junctions of the mouse heart and liver, J. Cell Biol. 33 (1967) C7–C12.
[19] J.D. Robertson, The occurrence of a subunit pattern in the unit membrane of the club ending in Mauthner cell synapses in goldfish brains, J. Cell Biol. 19 (1963) 201–221.
[20] E.L. Benedetti, P. Emmelot, Electron microscopic observations on negatively stained plasma membranes isolated from rat liver, J. Cell Biol. 26 (1965) 299–305.
[21] M.M. Dewey, L. Barr, Intercellular connections between smooth muscle cells: the nexus, Science 137 (1962) 670–672.
[22] D.A. Goodenough, J.-P. Revel, A fine structural analysis of intercellular gap junctions in the mouse liver, J. Cell Biol. 45 (1970) 272–290.
[23] N.S. McNutt, R.S. Weinstein, The ultrastructure of the nexus, A correlated thin-section and freeze-cleave study, J. Cell Biol. 47 (1970) 666–688.
[24] E.C. Beyer, D.A. Goodenough, D.L. Paul, The Connexins, a family of related gap junction proteins, in: E. Hertzberg, R. Johnson (Eds.), Gap Junctions, Alan R. Liss, Inc., New York, 1988, pp. 167–175.
[25] L.C. Milks, N.M. Kumar, R. Houghten, N. Unwin, N.B. Gilula, Topology of the 32-kd liver gap junction protein determined by site-directed antibody localizations, EMBO J. 7 (1988) 2967–2975.
[26] D.A. Goodenough, D.L. Paul, L. Jesaitis, Topological distribution of two connexin32 antigenic sites in intact and split rodent hepatocyte gap junctions, J. Cell Biol. 107 (1988) 1817–1824.
[27] D.L. Paul, Molecular cloning of cDNA for rat liver gap junction protein, J. Cell Biol. 103 (1986) 123–134.
[28] N.M. Kumar, N.B. Gilula, Cloning and characterization of human and rat liver cDNAs coding for a gap junction protein, J. Cell Biol. 103 (1986) 767–776.
[29] V.M. Unger, N.M. Kumar, N.B. Gilula, M. Yeager, Three-dimensional structure of a recombinant gap junction membrane channel, Science 283 (1999) 1176–1180.
[30] S.J. Fleishman, V.M. Unger, M. Yeager, N. Ben-Tal, A C(alpha) model for the transmembrane alpha helices of gap junction intercellular channels, Mol. Cell 15 (2004) 879–888.
[31] R. Bruzzone, T.W. White, D.L. Paul, Expression of chimeric connexins reveals new properties of the formation and gating of gap junction channels, J. Cell Sci. 107 (1994) 955–967.

[32] N. Unwin, Is there a common design for cell membrane channels? Nature 323 (1986) 12–13.
[33] C.I. Foote, L. Zhou, X. Zhu, B.J. Nicholson, The pattern of disulfide linkages in the extracellular loop regions of connexin32 suggests a model for the docking interface of gap junctions, J. Cell Biol. 140 (1998) 1187–1197.
[34] S. Ghoshroy, D.A. Goodenough, G.E. Sosinsky, Preparation, characterization, and structure of half gap junctional layers split with urea and EGTA, J. Membr. Biol. 146 (1995) 15–28.
[35] K. Willecke, J. Eiberger, J. Degen, D. Eckardt, A. Romualdi, M. Guldenagel, U. Deutsch, G. Sohl, Structural and functional diversity of connexin genes in the mouse and human genome, Biol. Chem. 383 (2002) 725–737.
[36] G.E. Sosinsky, Mixing of connexins in gap junction membrane channels, Proc. Natl. Acad. Sci. 92 (1995) 9210–9214.
[37] A. Kuraoka, H. Iida, T. Hatae, Y. Shibata, M. Itoh, T. Kurita, Location of gap junction proteins, connexins 32 and 26, in rat and guinea pig liver as revealed by quick-freeze, deep-etch immunoelectron microscopy, J. Histochem. Cytochem. 41 (1993) 971–980.
[38] M. Yeager, N.B. Gilula, Membrane topology and quaternary structure of cardiac gap junction ion channels, J. Mol. Biol. 223 (1992) 929–948.
[39] E.L. Hertzberg, A detergent independent procedure for the isolation of gap junctions from rat liver, J. Biol. Chem. 259 (1984) 9936–9943.
[40] J. Kistler, S. Bullivant, The connexon order in isolated lens gap junctions, J. Ultrastr. Res. 72 (1980) 27–38.
[41] M. Yeager, V. Unger, Culturing of mammalian cells expressing recombinant connexins and two-dimensional crystallization of isolation gap junctions, in: R. Bruzzone, C. Giaume (Eds.), Methods in Molecular Biology: Connexin Methods and Protocols, Humana Press, Totowa, NJ, 2001, pp. 77–89.
[42] G.M. Hand, D.J. Muller, B.J. Nicholson, A. Engel, G.E. Sosinsky, Isolation and characterization of gap junctions from tissue culture cells, J. Mol. Biol. 315 (2002) 587–600.
[43] J. Kistler, J. Bond, P. Donaldson, A. Engel, Two distinct levels of gap junction assembly in vitro, J. Struct. Biol. 110 (1993) 28–38.
[44] A.L. Harris, A. Walter, D. Paul, D.A. Goodenough, J. Zimmerberg, Ion channels in single bilayers induced by rat connexin32, Mol. Brain Res. 15 (1992) 269–280.
[45] J.X. Jiang, D.A. Goodenough, Heteromeric connexons in lens gap junction channels, Proc. Natl. Acad. Sci. 3 (1996) 1287–1291.
[46] K.A. Stauffer, The gap junction protein β1-connexin (connexin-32) and β2-connexin (connexin26) can form heteromeric hemichannels, J. Biol. Chem. 270 (1995) 6768–6772.
[47] K.A. Stauffer, N.M. Kumar, N.B. Gilula, N. Unwin, Isolation and purification of gap junction channels, J. Cell Biol. 115 (1991) 141–150.
[48] A. Oshima, T. Doi, K. Mitsuoka, S. Maeda, Y. Fujiyoshi, Roles of Met-34, Cys-64, and Arg-75 in the assembly of human connexin 26, Implication for key amino acid residues for channel formation and function, J. Biol. Chem. 278 (2003) 1807–1816.
[49] J. Kistler, K. Goldie, P. Donaldson, A. Engel, Reconstitution of native-type noncrystalline lens fiber gap junctions from isolated hemichannels, J. Cell Biol. 126 (1994) 1047–1058.
[50] D.A. Goodenough, Bulk isolation of mouse hepatocyte gap junctions. Characterization of the principle protein, connexin, J. Cell Biol. 61 (1974) 557–563.
[51] W.H. Evans, J.W. Gurd, Preparation and properties of nexus and lipid enriched vesicles from mouse liver plasma membranes, Biochem. J. 128 (1972) 691–700.
[52] E. Gogol, N. Unwin, Organization of connexons in isolated rat liver gap junctions, Biophys. J. 54 (1988) 105–112.
[53] L. Makowski, D.L.D. Caspar, D.A. Goodenough, W.C. Phillips, Gap junction structures III: The effect of variations in isolation procedures, Biophys. J. 37 (1982) 189–191.
[54] N. Hirokawa, J. Heuser, The inside and outside of gap junction membranes visualized by deep etching, Cell 30 (1982) 395–406.
[55] G.E. Sosinsky, T.S. Baker, D.L.D. Caspar, D.A. Goodenough, Correlation analysis of gap junction lattices, Biophys. J. 58 (1990) 1213–1226.
[56] D.R. Nelson, B.I. Halperin, Dislocation-mediated melting in two dimensions, Phys. Rev., B 19 (1979) 2457–2484.
[57] E.B. Sirota, G.S. Smith, C.R. Safinya, R.J. Plano, N.A. Clark, X-ray scattering studies of aligned, stacked surfactant membranes, Science 242 (1988) 1406–1409.
[58] J. Braun, J.R. Abney, J.C. Owicki, How a gap junction maintains its structure, Nature 310 (1984) 316–318.
[59] B. Malewicz, V.V. Kumar, R.G. Johnson, W.J. Baumann, Lipids in gap junction assembly and function, Lipids 25 (1990) 419–427.
[60] D. Henderson, H. Eibl, K. Weber, Structure and biochemistry of mouse hepatic gap junctions, J. Mol. Biol. 132 (1979) 193–218.
[61] T.S. Baker, D.L.D. Caspar, C.J. Hollingshead, D.A. Goodenough, Gap junction structures: IV. Asymmetric features revealed by low-irradiation microscopy, J. Cell Biol. 96 (1983) 204–216.
[62] D.A. Goodenough, W. Stoeckenius, Isolation of mouse hepatocyte gap junctions, Preliminary chemical characterization and X-ray diffraction, J. Cell Biol. 54 (1972) 646–656.
[63] G.E. Sosinsky, J.C. Jesior, D.L.D. Caspar, D.A. Goodenough, Gap junction structures VIII: Membrane cross-sections, Biophys. J. 53 (1988) 709–722.
[64] T.S. Baker, G.E. Sosinsky, D.L.D. Caspar, C. Gall, D.A. Goodenough, Gap junction structures VII. Analysis of connexon images obtained with cationic and anionic negative stains, J. Mol. Biol. 184 (1985) 81–98.
[65] G. Zampighi, P.N.T. Unwin, Two forms of isolated gap junctions, J. Mol. Biol. 135 (1979) 451–464.
[66] P.N.T. Unwin, P.D. Ennis, Two configurations of a channel-forming membrane protein, Nature 307 (1984) 609–613.
[67] D.L.D. Caspar, D.A. Goodenough, L. Makowski, W.C. Phillips, Gap junctions structures I: correlated electron microscopy and X-ray diffraction, J. Cell Biol. 74 (1977) 605–628.
[68] L.A. Amos, R. Henderson, P.N. Unwin, Three-dimensional structure determination by electron microscopy of two-dimensional crystals, Prog. Biophys. Mol. Biol. 39 (1982) 183–231.
[69] K.I. Swenson, J.R. Jordan, E.C. Beyer, D.L. Paul, Formation of gap junctions by expressions of connexins in *Xenopus* oocyte pairs, Cell 57 (1989) 145–155.
[70] A.L. Harris, Emerging issues of connexin channels: biophysics fills the gap, Q. Rev. Biophys. 34 (2001) 325–472.
[71] M. Yeager, B.J. Nicholson, Structure of gap junction intercellular channels, Curr. Opin. Struct. Biol. 6 (1996) 183–192.
[72] A.L. Harris, C.G. Bevans, Molecular selectivity of homomeric and heteromeric connexin channels, in: R. Werner (Ed.), Gap Junctions, IOS Press, Amsterdam, 1998.
[73] C.G. Bevans, M. Kordel, S.K. Rhee, A.L. Harris, Isoform composition of connexin channels determines selectivity among second messengers and uncharged molecules, J. Biol. Chem. 273 (1998) 2808–2816.
[74] F. Cao, R. Eckert, C. Elfgang, J.M. Nitsche, S.A. Snyder, D.F. Hülser, K. Willecke, B.J. Nicholson, A quantitative analysis of connexin-specific permeability differences of gap junctions expressed in HeLa transfectants and *Xenopus* oocytes, J. Cell Sci. 111 (1998) 31–43.
[75] E.B. Trexler, M.V.L. Bennett, T.A. Bargiello, V.K. Verselis, Voltage gating and permeation in a gap junction hemichannel, Proc. Natl. Acad. Sci. 93 (1996) 5836–5841.
[76] R.D. Veenstra, Size and selectivity of gap junction channels formed from different connexins, J. Bioenerg. Biomembr. 28 (1996) 327–337.
[77] J.-T. Zhang, B.J. Nicholson, The topological structure of connexin 26 and its distribution compared to connexin 32 in hepatic gap junctions, J. Membr. Biol. 139 (1994) 15–29.
[78] J.E. Rash, T. Yasumura, F.E. Dudek, J.I. Nagy, Cell-specific

expression of connexins and evidence of restricted gap junctional coupling between glial cells and between neurons, J. Neurosci. 21 (2001) 1983–2000.
[79] B. Risek, F.G. Klier, N.B. Gilula, Developmental regulation and structural organization of connexins in epidermal gap junctions, Dev. Biol. 164 (1994) 183–196.
[80] M. Falk, Connexin-specific distribution within gap junctions revealed in living cells, J. Cell Sci. 113 (2000) 4109–4120.
[81] D.W. Laird, K. Jordan, T. Thomas, H. Qin, P. Fistouris, Q. Shao, Comparative analysis and application of fluorescent protein-tagged connexins, Microsc. Res. Tech. 52 (2001) 263–272.
[82] M.M. Falk, U. Lauf, High resolution, fluorescence deconvolution microscopy and tagging with the autofluorescent tracers CFP, GFP, and YFP to study the structural composition of gap junctions in living cells, Microsc. Res. Tech. 52 (2001) 251–262.
[83] J.S. Wall, J. Hainfeld, Mass mapping by STEM, Annu. Rev. Biophys. Biophys. Chem. 15 (1986) 355–376.
[84] T.W. White, R. Bruzzone, S. Wolfram, D.L. Paul, D.A. Goodenough, Selective interactins among multiple connexin proteins expressed in the vertebrate lens: the second extracellular domain is a determinant of compatibility between connexins, J. Cell Biol. 125 (1994) 879–892.
[85] S. Haubrich, H.-J. Schwarz, F. Bukauskas, Incompatibility of connnexin 40 and 43 hemichannels in gap junctions between mammalian cells is determined by intracellular domains, Mol. Biol. Cell 7 (1996) 1995–2006.
[86] L. Makowski, D.L.D. Caspar, W.C. Phillips, D.A. Goodenough, Gap Junction structure: II. Analysis of the X-ray diffraction data, J. Cell Biol. 74 (1977) 629–645.
[87] T.T. Tibbitts, D.L.D. Caspar, W.C. Phillips, D.A. Goodenough, Diffraction diagnosis of protein folding in gap junction connexons, Biophys. J. 57 (1990) 1025–1036.
[88] P.N.T. Unwin, P.D. Ennis, Calcium-mediated changes in gap junction structure: evidence from the low angle X-ray pattern, J. Cell Biol. 97 (1983) 1459–1466.
[89] P.N.T. Unwin, G. Zampighi, Structure of the junction between communicating cells, Nature 283 (1980) 545–549.
[90] M. Cascio, E. Gogol, B.A. Wallace, The secondary structure of gap Junctions. Influence of isolation methods and proteolysis, J. Biol. Chem. 265 (1990) 2358–2364.
[91] G.A. Perkins, D.A. Goodenough, G.E. Sosinsky, Three-dimensional structure of the gap junction connexon, Biophys. J. 72 (1997) 533–544.
[92] G.E. Sosinsky, Image analysis of gap junction structures, Electron Microsc. Rev. 3 (1992) 59–76.
[93] D.J. Muller, G.M. Hand, A. Engel, G.E. Sosinsky, Conformational changes in surface structures of isolated connexin 26 gap junctions, EMBO J. 21 (2002) 3598–3607.
[94] M. Yeager, Structure of cardiac gap junction intercellular channels, J. Struct. Biol. 121 (1998) 231–245.
[95] L. Makowski, D.L.D. Caspar, W.C. Phillips, D.A. Goodenough, Gap junction structures V: Structural chemistry inferred from X-ray diffraction measurements on sucrose accessibility and trypsin susceptibility, J. Mol. Biol. 174 (1984) 449–481.
[96] D.B. Gros, B.J. Nicholson, J.-P. Revel, Comparative analysis of the gap junction protein from rat and liver: is there a tissue specificity of gap junctions, Cell 35 (1983) 539–549.
[97] V.M. Unger, N.M. Kumar, N.B. Gilula, M. Yeager, Projection structure of a gap junction membrane channel at 7 Å resolution, Nat. Struct. Biol. 4 (1997) 39–43.
[98] N.M. Kumar, D.S. Friend, N.B. Gilula, Synthesis and assembly of human β1 gap junctions in BHK cells by DNA transfection with the human β1 cDNA, J. Cell Sci. 108 (1995) 3725–3734.
[99] D.L. Boger, J.E. Patterson, X. Guan, B.F. Cravatt, R.A. Lerner, N.B. Gilula, Chemical requirements for inhibition of gap junction communication by the biologically active lipid oleamide, Proc. Natl. Acad. Sci. U. S. A. 95 (1998) 4810–4815.
[100] A. Cheng, D. Schweissinger, F. Dawood, N. Kumar, M. Yeager, Projection structure of full length connexin 43 by electron cryo-crystallography, Cell Commun. Adhes. 10 (2003) 187–191.
[101] J. Hoh, G.E. Sosinsky, J.-P. Revel, P.K. Hansma, Structure of the extracellular surface of the gap junction by atomic force microscopy, Biophys. J. 65 (1993) 149–163.
[102] M.V.L. Bennett, L.C. Barrio, T.A. Bargiello, D.C. Spray, E. Hertzberg, J.C. Saez, Gap junctions: new tools, new answers, new questions, Neuron 6 (1991) 305–320.
[103] N. Unwin, The structure of ion channels in membranes of excitable cells, Neuron 3 (1989) 665–676.
[104] R.S. Nunn, T.J. Macke, A.J. Olson, M. Yeager, Transmembrane alpha-helices in the gap junction membrane channel: systematic search of packing models based on the pair potential function, Microsc. Res. Tech. 52 (2001) 344–351.
[105] D.J. Barlow, J.M. Thornton, Helix geometry in proteins, J. Mol. Biol. 201 (1988) 601–619.
[106] T.M. Suchyna, L.X. Xu, F. Gao, C.R. Fourtner, B.J. Nicholson, Identification of a proline residue as a transduction element involved in voltage gating of gap junctions, Nature 365 (1993) 847–849.
[107] Y. Ri, J.A. Ballesteros, C.K. Abrams, S. Oh, V.K. Versalis, H. Weinstein, T.A. Bargiello, The role of a conserved proline residue in a mediating conformational changes associated with voltage gating of Cx32 gap junctions, Biophys. J. 76 (1999) 2887–2898.
[108] I.M. Skerrett, J. Aronowitz, J.H. Shin, G. Cymes, E. Kasperek, F.L. Cao, B.J. Nicholson, Identification of amino acid residues lining the pore of a gap junction channel, J. Cell Biol. 159 (2002) 349–360.
[109] S. Oh, Y. Ri, M.V.L. Bennett, E.B. Trexler, V.K. Verselis, T.A. Bargiello, Changes in permeability caused by connexin32 mutations underlie X-linked Charcot–Marie–Tooth Disease, Neuron 19 (1997) 927–938.
[110] X.-W. Zhou, A. Pfahnl, R. Werner, A. Hudder, A. Lianes, A. Luebke, G. Dahl, Identification of a pore lining segment in gap junction hemichannels, Biophys. J. 72 (1997) 1946–1953.
[111] D.B. Zimmer, C.R. Green, W.H. Evans, N.B. Gilula, Topological analysis of the major protein in isolated intact rat liver gap junctions and gap junction-derived single membrane structures, J. Biol. Chem. 262 (1987) 7751–7763.
[112] J. Kronengold, E.B. Trexler, F.F. Bukauskas, T.A. Bargiello, V.K. Verselis, Single-channel SCAM identifies pore-lining residues in the first extracellular loop and first transmembrane domains of Cx46 hemichannels, J. Gen. Physiol. 122 (2003) 389–405.
[113] G.A. Perkins, D.A. Goodenough, G.E. Sosinsky, Structural considerations for connexon docking, in: R. Werner (Ed.), Gap Junctions, IOS Press, Amsterdam, 1998, pp. 13–17.
[114] G.A. Perkins, D.A. Goodenough, G.E. Sosinsky, Formation of the gap junction intercellular channel requires a 30° rotation for interdigitating two apposing connexons, J. Mol. Biol. 277 (1998) 171–177.
[115] J.D. Batchelor, A. Olteanu, A. Tripathy, G.J. Pielak, Impact of protein denaturants and stabilizers on water structure, J. Am. Chem. Soc. 126 (2004) 1958–1961.
[116] S.A. John, J.-P. Revel, Connexin integrity is maintained by non-covalent bonds: intramolecular disulfide bonds link the extracellular domains in rat connexin-43, Biochem. Biophys. Res. Commun. 178 (1991) 1312–1328.
[117] G. Dahl, W. Nonner, R. Werner, Attempts to define functional domains of gap junction proteins with synthetic peptides, Biophys. J. 67 (1994) 1816–1822.
[118] C. Peracchia, A. Lazrak, L.L. Peracchia, Molecular models of channel interaction and gating in gap junctions, in: C. Peracchia (Ed.), Membrane Channels, Molecular and Cellular Physiology, Academic Press, New York, 1994, pp. 361–377.
[119] J.M. Gomez-Hernandez, M. de Miguel, B. Larrosa, D. Gonzalez, L.C. Barrio, Molecular basis of calcium regulation in connexin-32 hemichannels, Proc. Natl. Acad. Sci. U. S. A. 100 (2003) 16030–16035.

[120] G. Binnig, C.F. Quate, C. Gerber, Atomic force microscope, Phys. Rev. Lett. 56 (1986) 930–933.
[121] J.H. Hoh, R. Lal, S.A. John, J.-P. Revel, M.F. Arnsdorf, Atomic force microscopy and dissection of gap junctions, Science 235 (1991) 1405–1408.
[122] A. Engel, C.A. Schoenenberger, D.J. Muller, High resolution imaging of native biological sample surfaces using scanning probe microscopy, Curr. Opin. Struct. Biol. 7 (1997) 279–284.
[123] D.M. Czajkowsky, Z. Shao, Submolecular resolution of single macromolecules with atomic force microscopy, FEBS Lett. 430 (1998) 51–54.
[124] A. Engel, D.J. Muller, Observing single biomolecules at work with the atomic force microscope, Nat. Struct. Biol. 7 (2000) 715–718.
[125] A. Engel, Y. Lyubchenko, D. Muller, Atomic force microscopy: a powerful tool to observe biomolecules at work, Trends Cell Biol. 9 (1999) 77–80.
[126] B. Drake, C.B. Prater, A.L. Weisenhorn, S.A. Gould, T.R. Albrecht, C.F. Quate, D.S. Cannell, H.G. Hansma, P.K. Hansma, Imaging crystals, polymers, and processes in water with the atomic force microscope, Science 243 (1989) 1586–1589.
[127] D.J. Müller, A. Engel, The height of biomolecules measured with the atomic force microscope depends on electrostatic interactions, Biophys. J. 73 (1997) 1633–1644.
[128] J.H. Hoh, S.A. John, J.-P. Revel, Molecular cloning and characterization of a new member of the gap junction gene family, connexin-31, J. Biol. Chem. 266 (1991) 6524–6531.
[129] R. Lal, S.A. John, D.W. Laird, M.F. Arnsdorf, Heart gap junction preparations reveal hemiplaques by atomic force microscopy, Am. J. Physiol. 268 (1995) C968–C977.
[130] R. Lal, H. Lin, Imaging molecular structure and physiological function of gap junctions and hemijunctions by multimodal atomic force microscopy, Microsc. Res. Tech. 52 (2001) 273–288.
[131] R.E.M. Purnick, D.C. Benjamin, V.K. Verselis, T.A. Bargiello, Structure of the amino terminus of a gap junction protein, Arch. Biochem. Biophys. 381 (2000) 181–190.
[132] M. Delmar, K. Stergiopoulos, N. Homma, G. Calero, G. Morley, J.F. Ek-Vitorin, S.M. Taffet, A molecular model for the chemical regulation of connexin43 channels: the "ball and chain" hypothesis, in: C. Peracchia (Ed.), Gap Junctions, Molecular Basis of Cell Communication in Health and Disease, Academic Press, San Diego, 2000, pp. 223–248.
[133] H.S. Duffy, P.L. Sorgen, M.E. Girvin, P. O'Donnell, W. Coombs, S.M. Taffet, M. Delmar, D.C. Spray, pH-dependent intramolecular binding and structure involving Cx43 cytoplasmic domains, J. Biol. Chem. 277 (2002) 36706–36714.
[134] L. Zhou, E.M. Kasperek, B.J. Nicholson, Dissection of the molecular basis of pp60(v-src) induced gating of connexin 43 gap junction channels, J. Cell Biol. 144 (1999) 1033–1045.
[135] A. Pfahnl, G. Dahl, Gating of cx46 gap junction hemichannels by calcium and voltage, Pflugers Arch. 437 (1999) 345–353.
[136] A.P. Quist, S.K. Rhee, H. Lin, R. Lal, Physiological role of gap-junctional hemichannels: extracellular calcium-dependent isomotic volume regulation, J. Cell Biol. 148 (2000) 1063–10744.
[137] J. Thimm, A. Mechler, H. Lin, S. Rhee, R. Lal, Calcium dependent open-closed conformations and interfacial energy maps of reconstituted hemichannels, J. Biol. Chem. 280 (2005) 10646–10654.
[138] O. Spiga, A. Bernini, M. Scarselli, A. Ciutti, L. Bracci, L. Lozzi, B. Lelli, D. Di Maro, D. Calamandrei, N. Niccolai, Peptide–protein interactions studied by surface plasmon and nuclear magnetic resonances, FEBS Lett. 511 (2002) 33–35.
[139] Z. Salamon, M.F. Brown, G. Tollin, Plasmon resonance spectroscopy: probing molecular interactions within membranes, Trends Biochem. Sci. 24 (1999) 213–219.
[140] H.S. Duffy, M. Delmar, W. Coombs, S.M. Tafftet, E.L. Hertzberg, D.C. Spray, Functional demonstration of connexin-protein binding using surface plasmon resonance, Cell Adhes. Commun. 8 (2001) 225–229.
[141] A. Lombardi, F. Nastri, V. Pavone, Peptide-based heme-protein models, Chem. Rev. 101 (2001) 3165–3189.
[142] H. Zeng, E. Hawrot, NMR-based binding screen and structural analysis of the complex formed between alpha-cobratoxin and an 18-mer cognate peptide derived from the alpha 1 subunit of the nicotinic acetylcholine receptor from *Torpedo californica*, J. Biol. Chem. 277 (2002) 37439–37445.
[143] E. Katchalski-Katzir, R. Kasher, M. Balass, T. Scherf, M. Harel, M. Fridkin, J.L. Sussman, S. Fuchs, Design and synthesis of peptides that bind alpha-bungarotoxin with high affinity and mimic the three-dimensional structure of the binding-site of acetylcholine receptor, Biophys. Chem. 100 (2003) 293–305.
[144] V.K. Verselis, C.S. Ginter, T.A. Bargiello, Opposite voltage gating polarities of two closely related connexins, Nature 368 (1994) 348–351.
[145] G. Gaietta, T.J. Deerinck, S.R. Adams, J. Bouwer, O. Tour, D.W. Laird, G.E. Sosinsky, R.Y. Tsien, M.H. Ellisman, Multicolor and electron microscopic imaging of connexin trafficking, Science 296 (2002) 503–507.
[146] G.E. Sosinsky, G.M. Gaietta, G. Hand, T.J. Deerinck, A. Han, M. Mackey, S.R. Adams, J. Bouwer, R.Y. Tsien, M.H. Ellisman, Tetracysteine genetic tags complexed with biarsenical ligands as a tool for investigating gap junction structure and dynamics, Cell Commun. Adhes. 10 (2003) 181–186.
[147] S. Oh, S. Rivkin, Q. Tang, V.K. Verselis, T.A. Bargiello, Determinants of gating polarity of a connexin 32 hemichannel, Biophys. J. 87 (2004) 912–928.
[148] P.L. Sorgen, H.S. Duffy, S.M. Cahill, W. Coombs, D.C. Spray, M. Delmar, M.E. Girvin, Sequence-specific resonance assignment of the carboxyl terminal domain of Connexin43, J. Biomol. NMR 23 (2002) 245–246.
[149] P.L. Sorgen, H.S. Duffy, D.C. Spray, M. Delmar, pH-dependent dimerization of the carboxyl terminal domain of Cx43, Biophys. J. 87 (2004) 574–581.
[150] P.L. Sorgen, H.S. Duffy, P. Sahoo, W. Coombs, M. Delmar, D.C. Spray, Structural changes in the carboxyl terminus of the gap junction protein connexin43 indicates signaling between binding domains for c-Src and zonula occludens-1, J. Biol. Chem. 279 (2004) 54695–54701.
[151] K. Stergiopoulos, J.L. Alvarado, M. Mastroianni, J.F. Ek-Vitorin, S.M. Taffet, M. Delmar, Hetero-domain interactions as a mechanism for the regulation of connexin channels, Circ. Res. 84 (1999) 1144–1155.
[152] R.D. Veenstra, H.Z. Wang, D.A. Beblo, M.G. Chilton, A.L. Harris, E.C. Beyer, P.R. Brink, Selectivity of connexin-specific gap junctions does not correlate with channel conductance, Circ. Res. 77 (1995) 1156–1165.
[153] D.A. Beblo, R.D. Veenstra, Monovalent cation permeation through the connexin40 gap junction channel. Cs, Rb, K, Na, Li, TEA, TMA, TBA, and effects of anions Br, Cl, F, acetate, aspartate, glutamate, and NO3, J. Gen. Physiol. 109 (1997) 509–522.
[154] E.B. Trexler, F.F. Bukauskas, J. Krongengold, T.A. Bargiello, V.V. Verselis, The first extracellular loop domain is a major determinant of charge selectivity in connexin46 channels, Biophys. J. 79 (2000) 3036–3051.
[155] T.M. Suchyna, J.M. Nitsche, M. Chilton, A.L. Harris, R.D. Veenstra, B.J. Nicholson, Different ionic selectivities for connexins 26 and 32 produce rectifying gap junction channels, Biophys. J. 77 (1999) 2968–2987.
[156] P.R. Brink, M.M. Dewey, Evidence for fixed charge in the nexus, Nature 285 (1980) 101–102.
[157] H. Musa, E. Fenn, M. Crye, J. Gemel, E.C. Beyer, R. Veenstra, Amino terminal glutamate residues confer spermine sensitivity and affect voltage gating and channel conductance of rat connexin40 gap junctions, J. Physiol. 553 (2004) 863–878.

[158] C. Elfgang, R. Eckert, H. Lichtenberg-Fraté, A. Butterweck, O. Traub, R.A. Klein, D.F. Hülser, K. Willecke, Specific permeability and selective formation of gap junction channels in connexin-transfected HeLa cells, J. Cell Biol. 129 (1995) 805–817.
[159] J.M. Nitsche, H.C. Chang, P.A. Weber, B.J. Nicholson, A transient diffusion model yields unitary gap junctional permeabilities from images of cell-to-cell fluorescent dye transfer between *Xenopus* oocytes, Biophys. J. 86 (2004) 2058–2077.
[160] P.A. Weber, H.C. Chang, K.E. Spaeth, J.M. Nitsche, B.J. Nicholson, The permeability of gap junction channels to probes of different size is dependent on connexin composition and permeant-pore affinities, Biophys. J. 87 (2004) 958–973.
[161] X.Q. Gong, B.J. Nicholson, Size selectivity between gap junction channels composed of different connexins, Cell Commun. Adhes. 8 (2001) 187–192.
[162] T. Lawrence, W.H. Beers, N.B. Gilula, Transmission of hormonal stimulation by cell–cell communication, Nature 272 (1978) 501–506.
[163] R.W. Tsien, R. Weingart, Proceedings: cyclic AMP: cell-to-cell movement and inotropic effect in ventricular muscle, studied by a cut-end method, J. Physiol. 242 (1974) 95P–96P.
[164] J.D. Pitts, J.W. Simms, Permeability of junctions between animal cells intercellular transfer of nucleotides but not of macromolecules, Exp. Cell Res. 104 (1977) 153–163.
[165] A.C. Charles, C.C. Naus, D. Zhu, G.M. Kidder, E.R. Dirksen, M.J. Sanderson, Intercellular calcium signaling via gap junctions in glioma cells, J. Cell Biol. 118 (1992) 195–201.
[166] J.C. Saez, J.A. Conner, D.C. Spray, M.V. Bennett, Hepatocyte gap junctions are permeable to the second messenger, inositol 1,4,5-triphosphate and to calcium ions, Proc. Natl. Acad. Sci. 86 (1989) 2708–2712.
[167] A. Tabernero, C. Giaume, J.M. Medina, Endothelin-1 regulates glucose utilization in cultured astrocytes by controlling intercellular communication through gap junctions, Glia 16 (1996) 187–195.
[168] J. Alvarez, Transfer of material from cell to cell, Acta Physiol. Latinoam. 23 (1973) 597–598.
[169] G.S. Goldberg, A.P. Moreno, P.D. Lampe, Gap junctions between cells expressing connexin 43 or 32 show inverse permselectivity to adenosine and ATP, J. Biol. Chem. 277 (2002) 36725–36730.
[170] Y. Qu, G. Dahl, Function of the voltage gate of gap junction channels: selective exclusion of molecules, Proc. Natl. Acad. Sci. U. S. A. 99 (2002) 697–702.
[171] P. Bedner, H. Niessen, B. Odermatt, K. Willecke, H. Harz, A method to determine the relative cAMP permeability of connexin channels, Exp. Cell Res. 291 (2003) 25–35.
[172] M. Beltramello, V. Piazza, F.F. Bukauskas, T. Pozzan, F. Mammano, Impaired permeability to Ins(1,4,5)P3 in a mutant connexin underlies recessive hereditary deafness, Nat. Cell Biol. 7 (2005) 63–69.
[173] D.A. Doyle, J.M. Cabral, R.A. Pfuestzner, A. Kuo, J.M. Gulbis, S.L. Cohen, B.T. Chait, R. MacKinnon, The structure of the potassium channel: molecular basis of K+ conduction and selectivity, Science 280 (1998) 69–77.
[174] X. Hu, G. Dahl, Exchange of conductance and gating properties between gap junction hemichannels, FEBS Lett. 451 (1999) 113–117.
[175] A.P. Moreno, J.C. Saez, G.I. Fishman, D.C. Spray, Human connexin43 gap junction channels. Regulation of unitary conductances by phosphorylation, Circ. Res. 74 (1994) 1051–1057.
[176] S. Oh, C.K. Abrams, V.K. Verselis, T.A. Bargiello, Stoichiometry of transjunctional voltage-gating polarity reversal by a negative charge substitution in the amino terminus of a connexin32 chimera [see comments], J. Gen. Physiol. 116 (2000) 13–31.
[177] A.L. Harris, D.C. Spray, M.V. Bennett, Kinetic properties of a voltage-dependent junctional conductance, J. Gen. Physiol. 77 (1981) 95–117.
[178] L. Ebihara, V.M. Berthoud, E.C. Beyer, Distinct behavior of connexin56 and connexin46 gap junctional channels can be predicted from the behavior of their hemi-gap-junctional channels, Biophys. J. 68 (1995) 1796–1803.
[179] E.B. Trexler, F.F. Bukauskas, M.V. Bennett, T.A. Bargiello, V.K. Verselis, Rapid and direct effects of pH on connexins revealed by the connexin46 hemichannel preparation, J. Gen. Physiol. 113 (1999) 721–742.
[180] D.L. Beahm, J.E. Hall, Hemichannel and junctional properties of connexin 50, Biophys. J. 82 (2002) 2016–2031.
[181] M. Srinivas, J. Kronengold, F.F. Bukauskas, T.A. Bargiello, V.K. Verselis, Correlative studies of gating in Cx46 and Cx50 hemichannels and gap junction channels, Biophys. J. 88 (2004) 1725–1739.
[182] G. Dahl, E. Levine, Rabadan-Diehl, R. Werner, Cell/cell channel formation involves disulfide exchange, Eur. J. Biochem. 197 (1991) 141–144.
[183] G. Fishman, A. Moreno, D. Spray, L. Leinwand, Functional analysis of human cardiac gap junction channel mutants, Proc. Natl. Acad. Sci. 88 (1991) 3525–3529.
[184] A.P. Moreno, G.I. Fishman, D.C. Spray, Phosphorylation shifts unitary conductance and modifies voltage dependent kinetics of human connexin43 gap junction channels, Biophys. J. 62 (1992) 51–53.
[185] P.D. Lampe, E.M. TenBroek, J.M. Burt, W.E. Kurata, R.G. Johnson, A.F. Lau, Phosphorylation of connexin43 on serine368 by protein kinase C regulates gap junctional communication, J. Cell Biol. 149 (2000) 1503–1512.
[186] F.F. Bukauskas, V.K. Verselis, Gap junction channel gating, Biochim. Biophys. Acta 1662 (2004) 42–60.
[187] L.C. Barrio, T. Suchyna, T. Bargiello, L.X. Xu, R.S. Roginski, M.V.L. Bennett, B.J. Nicholson, Gap junctions formed by connexins 26 and 32 alone and in combination are differently affected by applied voltage, Proc. Natl. Acad. Sci. 88 (1991) 8410–8414.
[188] A. Revilla, M.V. Bennett, L.C. Barrio, Molecular determinants of membrane potential dependence in vertebrate gap junction channels, Proc. Natl. Acad. Sci. U. S. A. 97 (2000) 14760–14765.
[189] F.F. Bukauskas, R. Weingart, Voltage-dependent gating of single gap junction channels in an insect cell line, Biophys. J. 67 (1994) 613–625.
[190] A. Pfahnl, G. Dahl, Localization of a voltage gate in connexin46 gap junction hemichannels, Biophys. J. 75 (1998) 2323–2331.
[191] F.F. Bukauskas, A. Bukauskiene, M.V. Bennett, V.K. Verselis, Gating properties of gap junction channels assembled from connexin43 and connexin43 fused with green fluorescent protein, Biophys. J. 81 (2001) 137–152.
[192] J.M. Anumonwo, S.M. Taffet, H. Gu, M. Chanson, A.P. Moreno, M. Delmar, The carboxyl terminal domain regulates the unitary conductance and voltage dependence of connexin40 gap junction channels, Circ. Res. 88 (2001) 666–673.
[193] G.E. Morley, S.M. Taffet, M. Delmar, Intramolecular interactions mediate pH regulation of connexin43 channels, Biophys. J. 70 (1996) 1294–1302.
[194] T. Hoshi, W.N. Zagoota, R.W. Aldrich, Biophysical and molecular mechanisms of Shaker potassium channel inactivation, Science 250 (1990) 533–538.
[195] J.F. Ek-Vitorin, G. Calero, G.E. Morley, W. Coombs, S.M. Taffet, M. Delmar, pH regulation of connexin43: molecular analysis of the gating particle, Biophys. J. 71 (1996) 1273–1284.
[196] J.F. Ek, M. Delmar, R. Rerzova, S.M. Taffet, Role of histidine 95 on pH gating of the cardiac gap junction protein Connexin43, Circ. Res. 74 (1994) 1058–1064.
[197] X. Wang, L. Li, L.L. Peracchia, C. Peracchia, Chimeric evidence for a role of the connexin cytoplasmic loop in gap junction channel gating, Pflugers Arch. 431 (1996) 844–852.
[198] X.G. Wang, C. Peracchia, Connexin 32/38 chimeras suggest a role for the second half of inner loop in gap junction gating by low pH, Am. J. Physiol. 271 (1996) C1743–C1749.
[199] X.G. Wang, C. Peracchia, Positive charges of the initial C-terminus

domain of Cx32 inhibit gap junction gating sensitivity to CO_2, Biophys. J. 73 (1997) 798–806.
[200] C.G. Bevans, A.L. Harris, Regulation of connexin channels by pH. Direct action of the protonated form of taurine and other aminosulfonates, J. Biol. Chem. 274 (1999) 3711–3719.
[201] B.J. Nicholson, L. Zhou, F. Cao, H. Zhu, Y. Chen, Diverse molecular mechanisms of gap junction channel gating, in: R. Werner (Ed.), Gap Junctions, IOS Press, Amsterdam, 1998, pp. 3–7.
[202] C.D. Cooper, P.D. Lampe, Casein kinase 1 regulates connexin-43 gap junction assembly, J. Biol. Chem. 277 (2002) 44962–44968.
[203] P.D. Lampe, Analyzing phorbol ester effects on gapjunctional communication: a dramatic inhibition of assembly, J. Cell Biol. 127 (1994) 1895–1905.
[204] A.D. Martinez, V. Hayrapetyan, A.P. Moreno, E.C. Beyer, A carboxyl terminal domain of connexin43 is critical for gap junction plaque formation but not for homo- or hetero-oligomerization, Cell Commun. Adhes. 10 (2003) 323–328.
[205] M.A. Thomas, N. Zosso, I. Scerri, N. Demaurex, M. Chanson, O. Staub, A tyrosine-based sorting signal is involved in connexin43 stability and gap junction turnover, J. Cell Sci. 116 (2003) 2213–2222.
[206] T.A. Nguyen, D.L. Boyle, L.M. Wagner, T. Shinohara, D.J. Takemoto, LEDGF activation of PKC gamma and gap junction disassembly in lens epithelial cells, Exp. Eye Res. 76 (2003) 565–572.
[207] P.D. Lampe, W.E. Kurata, B.J. Warn-Cramer, A.F. Lau, Formation of a distinct connexin43 phosophoisoform in mitotic cells is dependent upon p34cdc2 kinase, J. Cell Sci. 111 (1998) 833–841.
[208] M.M. Atkinson, A.S. Menko, R.G. Johnson, R. Sheppard, J.D. Sheridan, Rapid and reversible reduction of junctional permeability in cells infected with a temperature-sensitive mutant of avian sarcoma virus, J. Cell Biol. 91 (1981) 573–578.
[209] K.I. Swenson, H. Piwnica-Worms, H. McNamee, D.L. Paul, Tyrosine phosphorylation of the gap junction protein connexin43 is required for the pp60v-src-induced inhibition of communication, Cell Regul. 1 (1990) 989–1002.
[210] R. Lin, B.J. Warn-Cramer, W.E. Kurata, A.F. Lau, v-Src phosphorylation of connexin 43 on Tyr247 and Tyr265 disrupts gap junctional communication, J. Cell Biol. 154 (2001) 815–827.
[211] B.J. Warn-Cramer, P.D. Lampe, W.E. Kurata, M.Y. Kanemitsu, L.W. Loo, W. Eckhart, A.F. Lau, Characterization of the mitogen-activated protein kinase phosphorylation sites on the connexin-43 gap junction protein, J. Biol. Chem. 271 (1996) 3779–3786.
[212] M.Y. Kanemitsu, L.W. Loo, S. Simon, A.F. Lau, W. Eckhart, Tyrosine phosphorylation of connexin 43 by v-Src is mediated by SH2 and SH3 domain interactions, J. Biol. Chem. 272 (1997) 22824–22831.
[213] N. Homma, J.L. Alvarado, W. Coombs, K. Stergiopoulos, S.M. Taffet, A.F. Lau, M. Delmar, A particle-receptor model for the insulin-induced closure of connexin43 channels, Circ. Res. 83 (1998) 27–32.
[214] M. Yeager, B.J. Nicholson, Structure and biochemistry of gap junctions, in: E.L. Hertzberg (Ed.), Gap Junctions, JAI Press, Connecticut, 2000, pp. 31–98.
[215] D.L. Beahm, G.G. Gaietta, A. Chandrasekhar, G.M. Hand, A. Smock, A. Oshima, B.J. Nicholson, G.E. Sosinsky, A closed gap junction channel state caused by a single site mutation in the 3rd transmembrane helix, Microsc. Microanal. 10 (Suppl. 2) (2004) 1498–1499.
[216] D. Locke, N. Perusinghe, T. Newman, H. Jayatilake, W.H. Evans, P. Monaghan, Developmental expression and assembly of connexins into homomeric and heteromeric gap junction hemichannels in the mouse mammary gland, J. Cell. Physiol. 183 (2000) 228–237.
[217] M.M. Falk, L.K. Buehler, N.M. Kumar, N.B. Gilula, Cell-free synthesis and assembly of connexins into functional gap junction membrane channels, EMBO J. 16 (1997) 2703–2716.
[218] D.S. He, J.X. Jiang, S.M. Taffet, J.M. Burt, Formation of heteromeric gap junction channels by connexins 40 and 43 in vascular smooth muscle cells, Proc. Natl. Acad. Sci. U. S. A. 96 (1999) 6495–6500.
[219] A.D. Martinez, V. Hayrapetyan, A.P. Moreno, E.C. Beyer, Connexin43 and connexin45 form heteromeric gap junction channels in which individual components determine permeability and regulation, Circ. Res. 90 (2002) 1100–1107.
[220] P.R. Brink, K. Cronin, K. Banach, E. Peterson, E.M. Westphale, K.H. Seul, S.V. Ramanan, E.C. Beyer, Evidence for heteromeric gap junction channels formed from rat connexin43 and human connexin37, Am. J. Physiol. 273 (1997) C1386–C1396.
[221] V. Lagree, K. Brunschwig, P. Lopez, N.B. Gilula, G. Richard, M.M. Falk, Specific amino-acid residues in the N-terminus and TM3 implicated in channel function and oligomerization compatibility of connexin43, J. Cell Sci. 116 (2003) 3189–3201.
[222] B.J. Nicholson, Gap junctions—from cell to molecule, J. Cell Sci. 116 (2003) 4479–4481.
[223] J. Maza, J. DasSarma, M. Kova, Defining a minimal motif required to prevent connexin oligomerization in the endoplasmic reticulum. J. Biol. Chem. (in press).